 doi:10.20944/preprints202206.0422.v1

Article

Hydrochemistry of Medium-size Pristine Rivers in Boreal and Subarctic Zone: Disentangling Effect of Landscape Parameters across A Permafrost, Climate and Vegetation Gradient

Oleg S. Pokrovsky[1]*, Artem G. Lim[2], Ivan A. Krickov[2], Mikhail K. Korets[3], Liudmila S. Shirokova[1,4] and Sergey N. Vorobyev[2]

[1] GET UMR 5563 CNRS University of Toulouse (France), 14 Avenue Edouard Belin, 31400 Toulouse, France
[2] BIO-GEO-CLIM Laboratory, Tomsk State University, Lenina av., 36, Tomsk, Russia
[3] V.N. Sukachev Institute of Forest of the Siberian Branch of RAS, Krasnoyarsk, 660036, Russia
[4] N.P. Laverov Federal Center for Integrated Arctic Research, UrB Russian Academy of Science, 23 Nab Severnoi Dviny, Arkhangelsk, Russia
*Corresponding author: oleg@get.obs-mip.fr or oleg.pokrovsky@get.omp.eu

Abstract: Towards a better understanding of vegetation, permafrost, climate, landscape and lithology control on major and trace element (including macro and micro-nutrients and toxicants) transport in riverine systems, we studied two medium size (100-150 thousand km^2 watershed area) pristine rivers (Taz and Ket) of boreal and subarctic zone, western Siberia. Choosing the river basins of very low population density (< 1 people km^{-2}) in the absence of any industrial or agricultural activity allowed testing the sole effect of natural factors and long-range atmospheric transfer on hydrochemistry of riverine solutes during the open water period. In the permafrost-bearing Taz River (main stem and 17 tributaries), sizable control of vegetation on element concentration was revealed. In particular, light coniferous and broadleaf mixed forest controlled DOC, and some nutrients (NO_2, NO_3, Mn, Fe, Mo, Cd, Ba); deciduous needleleaf forest positively correlated with macronutrients (PO_4, P_{tot}, Si, Mg, P, Ca) and Sr, and dark needle-leaf forest impacted N_{tot}, Al and Rb. Organic C stock in the upper 30-100 cm soil positively correlated with Be, Mn, Co, Mo, Cd, Sb, and Bi. The lithological control was generally poorly pronounced, due to abundant peat deposits overlaying the mineral strata. However, cretaceous carbonate mineral-bearing sedimentary deposits positively impacted the pH and concentration of Si, Mg, Ca and Cs. In the Ket River basin (large right tributary of the Ob River), we revealed the correlations between the phytomass stock at the watershed and alkaline-earth metals and U concentration in the river water. This control was weakly pronounced during high-water period (spring flood) and mostly evidenced during summer low water period.

The pairwise correlations between elements in both river systems demonstrated two group of solutes – (1) positively correlated with DIC (S.C., Si, alkalis (Li, Na), alkaline-earth metals (Mg, Ca, Sr, Ba) and U); this link was originated from groundwater feeding of the river when the labile elements were leached from soluble minerals such as carbonates, and (2) positively correlated with DOC (trivalent (Sc, Al, Ga, Y, REE), tetravalent (Ti, Zr, Hf, Th) and other (Be, Cr, Nb) hydrolysates, Se and Cs), reflecting element mobilization from upper silicate mineral soil profile and plant litter, strongly facilitated by their colloidal status, even for low-mobile geochemical tracers. The observed DOC vs DIC control on riverine transport of low-soluble and highly mobile elements, respectively is also consistent with former observations in both lotic and lentic inland waters of the WSL as well as in soil waters and ice.

The Principal Component Analysis demonstrated three main factors potentially controlling the major and TE concentration variations. The first factor, responsible for 26 % of overall variation, included aluminum and other low mobile trivalent and tetravalent hydrolysates, Be, Cr, Nb, and elements strongly complexed with DOM such as Cu and Se. This factor presumably reflected the presence of organo-mineral colloids, being positively affected by the proportion of forest and organic C in soils of the watershed. The 2nd factor (14 % variation) likely represented a combined effect of productive litter in larch forest growing on carbonate-rich rocks and groundwater feeding of the rivers and acted on labile Na, Mg, Si, Ca, P and Fe(II), but also DOC, micronutrients (Zn, Rb, Ba) and phytomass at the watershed. Finally, the third factor, although exhibited limited explanation capacity, was strongly linked to pH, specific conductivity, DIC, Sr, and U and clearly marked a direct impact of bicarbonate-rich, slightly mineralized waters that reside in surface and subsurface reservoirs containing carbonate minerals.

Keywords: metals; trace elements; landscape; permafrost; river; watershed; boreal

---

1. Introduction

Climate change, which is mostly pronounced in high latitudes, strongly impacts the chemistry of rivers and streams and can bring yet unknown consequences on carbon, nutrient and metal export from land to ocean thus enhancing the retroactive link to climate change drivers [1-4]. This is especially true for pristine permafrost-bearing territories located at high latitudes and containing sizable amount of carbon in the form of peat, organic litter and vegetation. One of the best studied example is Western Siberian Lowland (WSL), located in the gradient of climate and permafrost zones at essentially the same lithological background, minimal variations in river runoff and relief and moderate to negligible anthropogenic activity. The interest of the WSL is that it contains huge peat resources and presents rather shallow, essentially discontinuous to sporadic/isolated permafrost, highly vulnerable to thawing [5-10]. For this relatively large territory (2 million km^2), extensive studies of small [11-19] and large [20] river dissolved, colloidal and particulate load, chemical composition of soil ice and suprapermafrost waters [21-24] and gaseous regime of rivers and lakes [25-27] have been performed. However, the majority of these studies except that of the Ob River [20] dealt with single site sampling of a given river, without addressing the spatial variability of riverine solutes within a watershed. This is a clear shortcomings of current state of knowledge of western Siberian rivers, because without sufficient spatial coverage, one cannot test the impact of various landscape factors on water hydrochemistry within the same river basin.

Towards better understanding of land cover control on riverine C, nutrient and metal transport, here we chose 2 medium size rivers of western Siberia, Taz ($S_{watershed}$ = 150,000 km^2) and Ket ($S_{watershed}$ = 95,000 km^2) located within permafrost-bearing forest-tundra/tundra and permafrost-free taiga biomes, respectively. Both rivers drain through similar sedimentary deposits overlayed by peatland and forest/tundra; they are virtually pristine (population density < 1 people km^{-2}) and have no industrial or agricultural activity on their watershed. Within the on-going drastic climate change in Siberia, the southern river (Ket) can be considered as an extreme case of long-term transformation of the northern River (Taz) in case of complete disappearance of discontinuous permafrost and northward migration of the taiga forest. Therefore, our primary objective in this work was to test the impact of climate and land cover parameters (permafrost, vegetation, water coverage, soil organic carbon, and lithology), on carbon, major and trace element concentration in the main stem and tributaries of each river separately and when considering them together, across contrasting climate/permafrost zones. We anticipate that, via employing similar approach for two sufficiently contrasting and yet representative river basin of the WSL, we can provide essential information for coupled land – river C, nutrient and metal fluxes for climate modeling of the region and to foresee future, long-term changes in much large territory of strongly understudied permafrost-affected Eurasian lowlands, which includes North Siberia, Anabar, Kolyma and Yana-Indigirka lowlands, with an overall territory more than 2 million km^2.

2. Study site and methods

2.1. Ket River basin

We sampled the Ket River main stem and its 26 tributaries during the peak of the spring flood and the end of summer baseflow. The catchment area of sampled watersheds ranged from 94,000 km² (Ket's mouth) to 20 km² (smallest tributary). The studied watersheds presented rather similar lithology, climate and vegetation, given its generally West – East orientation, **Fig. 1**; ref. 28). The Ket River basin (right tributary of the Ob River) is poorly accessible and can be considered as essentially pristine comprising about 50 % forest and 40 % of wetlands while having virtually negligible agricultural and forestry activity. The river basin is poorly populated (0.27 person km^{-2}) and, compared to left tributaries of the Ob River, lacks road infrastructure due to absence of hydrocarbon exploration activity. We therefore consider this river as a model one for medium size rivers of the boreal zone of western Siberia Lowland covered by forests and bogs. As such, the results on river water hydrochemistry obtained from this watershed can be extrapolated to much larger territory, comprising several million km^2 of permafrost-free taiga forest and bog biome, extending over 3000 km between the left tributaries of the Enisey River in the east and Finland in the west. The mean annual air temperatures (MAAT) of the Ket River basin is -0.75±0.15 °C and the mean annual precipitation is 520±20 mm y^{-1}. The lithology is represented by silts and sands with carbonate concretions overlayed by quaternary deposits (loesses, fluvial, glacial and lacustrine deposits). The dominant soils are podzols in forest areas and histosols in peat bog regions.

Preprints (www.preprints.org) | NOT PEER-REVIEWED | Posted: 30 June 2022 doi:10.20944/preprints202206.0422.v1

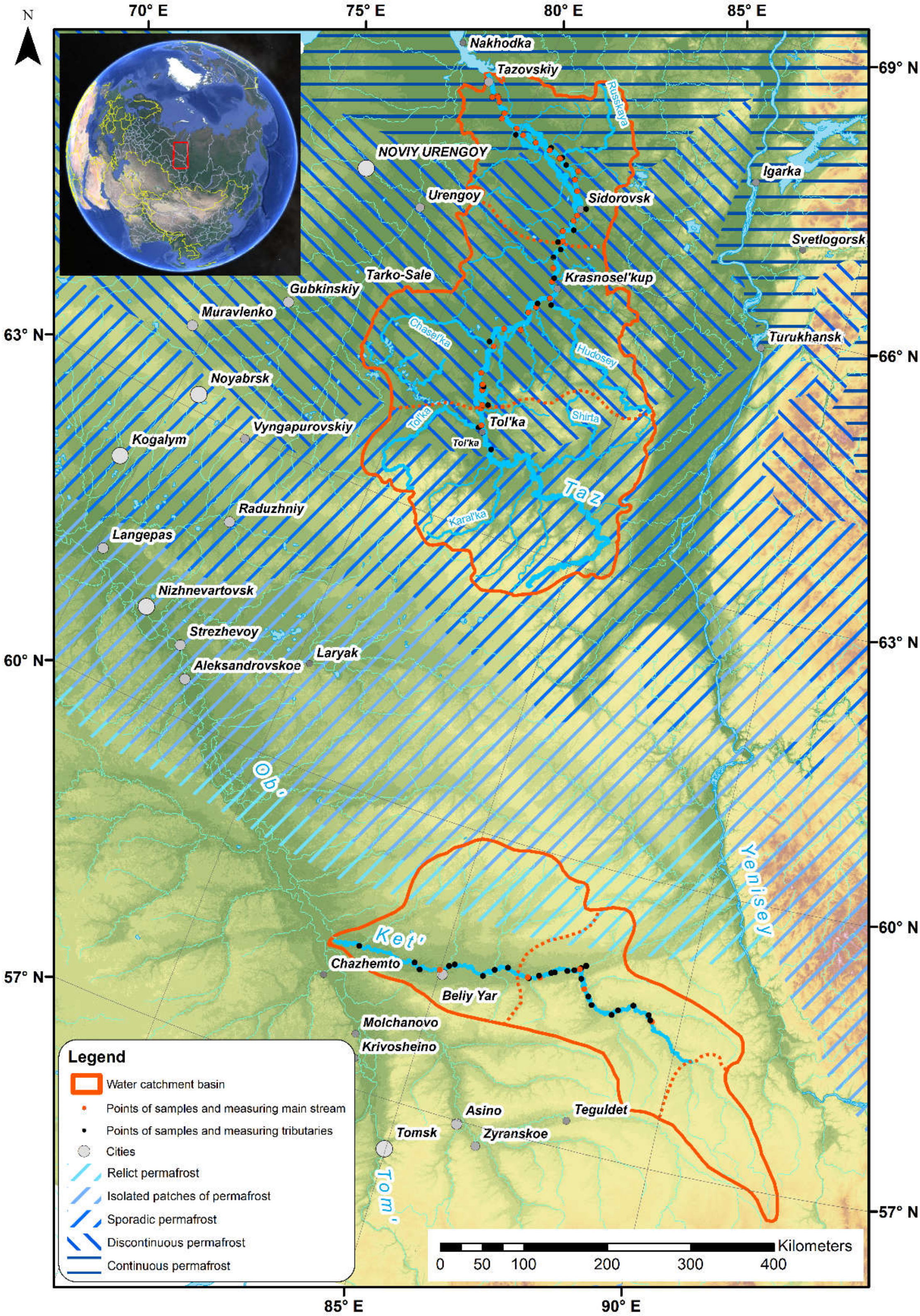

Figure 1. Map of the two studied river basins (Taz in the north and Ket in the south). The sampling points of the main stem and tributaries are shown by red and black circles, respectively.

2.2. Taz River basin

The Taz River sampled in this work included the main stem and its 17 tributaries whose catchment area ranged from 149,000 km² at the Taz's mouth to 25 km² of smallest sampled tributary. Alike the Ket River basin, all sampled catchments exhibited similar lithology (clays, silts and sands overlayed by quaternary loesses, fluvial, glacial and lacustrine deposits), but more contrasting climate and vegetation due to its North to South orientation (**Fig. 1**). The MAAT ranges from -4.6 °C in the headwaters (Tolka village) to -5.4 °C in the low reaches (Tazovskiy town). The mean annual precipitation is 500 mm y^{-1} in the central part of the basin (Krasnoselkup) and 600 mm y^{-1} in the low reaches of the Taz River. Given its landscape and climate features, the Taz River basin includes: 1) the upper (southern) part ("headwaters") which comprises 400-800 km upstream of the river mouth, where the permafrost is sporadic to discontinuous and the dominant vegetation is forest-tundra and taiga, and 2) the low reaches (northern) part, located 0-400 km upstream of the mouth where the permafrost is continuous to discontinuous and the dominant biome is tundra and forest-tundra.

2.3. Sampling

For the Ket River, the peak of annual discharge in 2019 occurred in the end of May whereas in August, the discharge was 3 to 5 times lower. From May 18 to May 28, 2019, and from August 30 to September 2, 2019, we started the boat trip in the middle course of the Ket River (Beliy Yar), and moved, first, 475 km upstream the Ket river till its most headwaters, and then moved 834 km downstream till the river mouth. We stopped each 50 km along the Ket River and sampled for major hydrochemical parameters, suspended matter and bacteria. We also moved several km upstream of selected tributaries to sample for river hydrochemistry.

In the Taz River, the peak of annual discharge in 2019 occurred in the middle of June (5600 m^3 s^{-1}; in August, the discharge was 5 times lower). Therefore, the month of July (average discharge is 2300 m^3 s^{-1} ; range 1920 – 3370 m^3 s^{-1}) can be considered as the end of spring flood period. From July 12 to July 16, 2019 we moved 800 km downstream the Taz River from its most headwaters (Tolka village) to the low reaches (Tazovskiy town). We stopped each ~50 to 100 km of the boat route and sampled for hydrochemical parameters, river suspended matter and total bacterial number of the main stem. For sampling the tributaries, we moved 500-1500 m upstream of the confluence zone.

2.4. Analyses

The dissolved oxygen (CellOx 325; accuracy of ±5%), specific conductivity (TetraCon 325; ±1.5%), and water temperature (±0.2 °C) were measured in-situ at 20 cm depth using a WTW 3320 Multimeter. The pH was measured using portable Hanna instrument via combined Schott glass electrode calibrated with NIST buffer solutions (4.01, 6.86 and 9.18 at 25°C), with an uncertainty of 0.01 pH units. The river water was sampled in pre-cleaned polypropylene bottle from 20-30 cm depth in the middle of the river and immediately filtered through disposable single-use sterile Sartorius filter units (0.45 μm pore size). The first 20 mL of filtrate was discarded. The DOC and Dissolved Inorganic Carbon (DIC) were determined by a Shimadzu TOC-VSCN Analyzer (Kyoto, Japan) with an uncertainty of 3% and a detection limit of 0.1 mg/L. Blanks of MilliQ water passed through the filters demonstrated negligible release of DOC from the filter material. The SUVA was measured via ultraviolet absorbance at 254 nm using a 10-mm quartz cuvette on a Bruker CARY-50 UV-VIS spectrophotometer.

The concentrations of C and N in suspended material (Particulate Organic Carbon and Nitrogen (POC and PON, respectively)) were determined via filtration of 1 to 2 L of freshly collected river water (at the river bank or in the boat) with pre-weighted GFF filters (47 mm, 0.8 μm) and Nalgene 250-mL polystyrene filtration units using a Mityvac® manual vacuum pump. Particulate C and N were measured using catalytic combustion with Cu-O at 900°C with an uncertainty of ≤ 0.5% using Thermo Flash 2000 CN Analyzer at EcoLab, Toulouse. The samples were analyzed before and after 1:1 HCl treatment to distinguish between total and inorganic C; however the ratio of $C_{organic}$: $C_{carbonate}$ in the river suspended matter (RSM) was always above 20 and the contribution of carbonate C to total C in the RSM was equal in average 0.3±0.3% (2 s.d., n = 30).

Total microbial cell concentration was measured after sample fixation in glutaraldehyde, by a flow cytometry (Guava® EasyCyteTM systems, Merck). Cells were stained using 1 μL of a 10 times diluted SYBR GREEN solution (10000x, Merck), added to 250 μL of each sample before analysis. Particles were identified as cells based on green fluorescence and forward scatter [29].

All analytical approaches used in this study for major and trace element analyses followed methods developed for western Siberian organic-rich surface waters [17, 30, 31]. The samples were preserved via refrigeration 1 month prior to analysis. Major anion (Cl, SO_4^{2-}) concentrations were measured by ion chromatography (HPLC, Dionex ICS 2000) with an uncertainty of 2%. International certified samples ION, PERADE, and RAIN were used for validation of the analyses. Major cations (Ca, Mg, Na, K), Si, and ~40 trace elements were determined with an Agilent iCap Triple Quad (TQ) ICP MS using both argon and helium modes to diminish interferences. About 3 μg L^{-1} of In and Re were added as internal standards along with 3 various external standards. Detection limits of TE were determined as 3× the blank concentration. The typical uncertainty for elemental concentration measurements ranged from 5-10 % at 1-1000 μg/L to 10-20 % at 0.001 – 0.1 μg/L. The MilliQ field blanks were collected and processed to monitor for any potential contamination introduced by our sampling and handling procedures. The SLRS-6 (Riverine Water Reference Material for Trace Metals certified by the National Research Council of Canada) was used to check the accuracy and reproducibility of analyses [32, 33]. Only those elements that exhibited good agreement between replicated measurements of SLRS-6 and the certified values (relative difference < 15%) are reported in this study.

2.5. Landscape parameters and water surface area of the Ket and Taz River basin

The physio-geographical characteristics of the Ket and Taz tributaries and several sampling points of the main stem of both rivers were determined by applying available digital elevation model (DEM GMTED2010), soil, vegetation and lithological maps. The landscape parameters were typified using TerraNorte Database of Land Cover of Russia (ref. 34; http://terranorte.iki.rssi.ru). This included various type of forest (evergreen, deciduous, needleleaf/broadleaf), grassland, tundra, wetlands, water bodies and riparian zones. The climate parameters the watershed were obtained from CRU grids data (1950-2016) [35] and NCSCD data (ref 36; doi:10.5879/ecds/00000001), respectively, whereas the biomass and soil OC content were obtained from BIOMASAR2 [37] and NCSCD databases. The lithology layer was taken from GIS version of Geological map of the Russian Federation (scale 1 : 5 000 000, http://www.geolkarta.ru/).

2.6. Data analysis

Element concentrations for all dataset were tested for normality using a Shapiro-Wilk test. In case of the data were not normally distributed, we used non-parametric statistics. Comparisons of major and trace element concentration in the main stem and the tributaries during two sampling seasons (Ket) and summer baseflow (Taz) were conducted using a non-parametric Mann Whitney test at a significance level of 0.05. For comparison of unpaired data, a non-parametric H-criterion Kruskal-Wallis test was used to reveal the differences between different seasons and between the main stem and tributaries. The Pearson rank order correlation coefficient ($p < 0.05$) was used to determine the relationship between major and trace element concentrations and main landscape parameters of several points of the main stem and all tributaries, as well as other potential drivers of TE concentrations in the river water such as pH, O_2, water temperature, specific conductivity, DOC, SUVA (aromaticity), DIC, Fe, Al, particulate carbon and nitrogen, and total bacterial number.

Preprints (www.preprints.org) | NOT PEER-REVIEWED | Posted: 30 June 2022 doi:10.20944/preprints202206.0422.v1

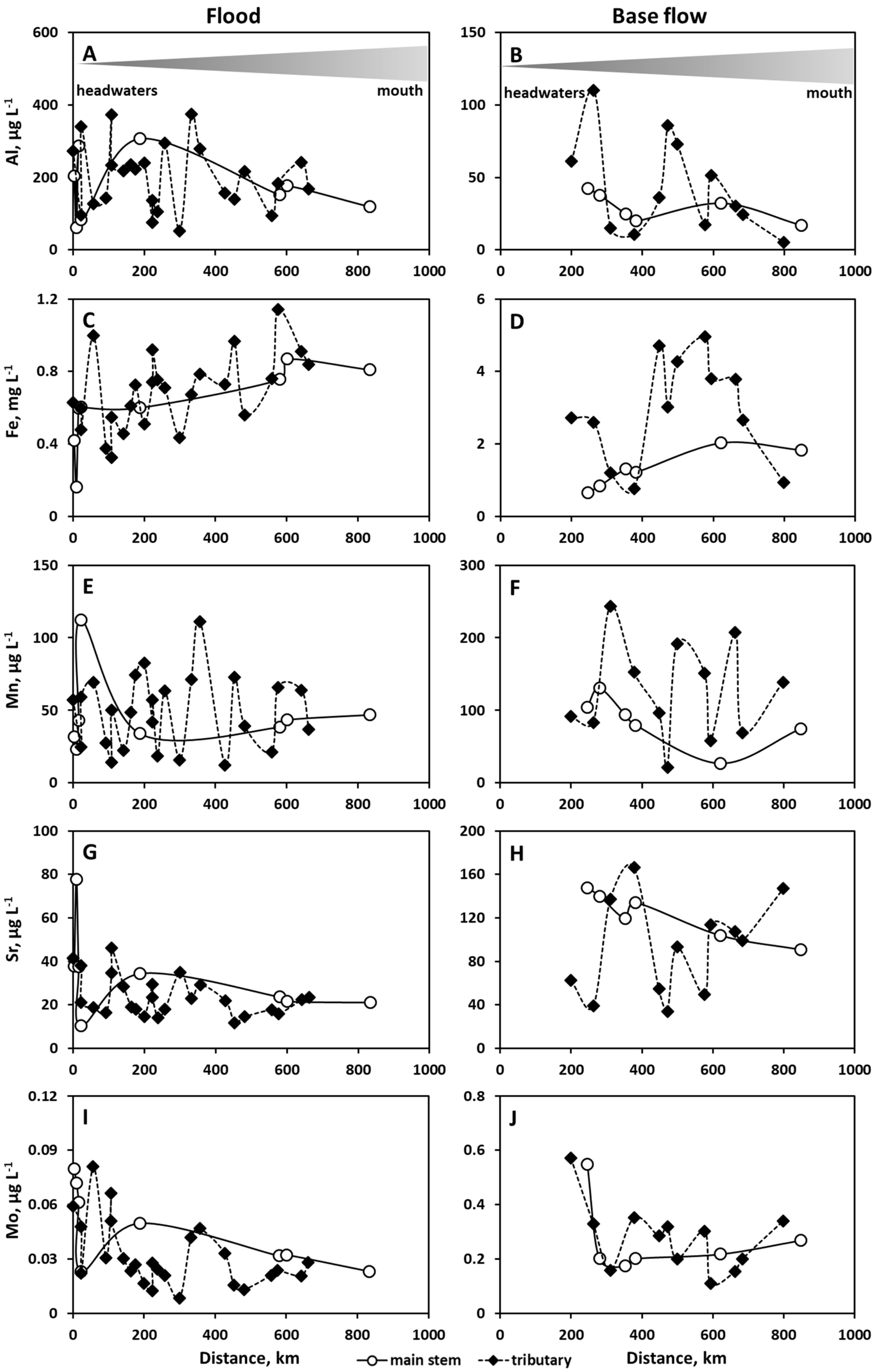

Figure 2. Al (A, B), Fe (C, D), Mn (E, F), Sr (G, H) and Mo (I, G) concentration in the Ket River main stem and tributaries during spring flood (left column) and summer baseflow (right column).

Preprints (www.preprints.org) | NOT PEER-REVIEWED | Posted: 30 June 2022 doi:10.20944/preprints202206.0422.v1

3. Results and Discussion

3.1. Spatial and seasonal variation of elements in the Ket River and control of river hydrochemistry by landscape parameters.

All the primary data on dissolved (< 0.45 µm) element concentration in both rivers together with relevant landscape parameters of the sampling points are available from the Mendeley Repository [28]. The spatial variations of element concentration in the main stem and tributaries of the Ket River were rather low compared to the differences between two seasons. This is illustrated by a plot of several major and trace elements along the full length of the river basin (**Fig. 2 A-E**), and further confirmed by a Mann-Whitney U test (**Table S1** of the Supplement) which shows that the maximal differences in element concentrations are observed between seasons in both the main stem and the tributaries compared to the differences between the main stem and the tributaries for the same season. This allowed to calculate the mean concentrations of elements across the full length of the main stem and among all tributaries for each seasons (**Fig. S1** and **Table S2** of the Supplement). Analyses of the differences in element concentration between the flood and the baseflow allowed distinguishing three group of elements as illustrated for selected elements in **Fig. 3**. The first groups comprised elements having a factor of 2 to 10 higher concentrations in both main stem of the Ket River and tributaries during spring flood compared to summer baseflow which included DOC, low soluble low mobile 'lithogenic' hydrolysates Be, Al, Ti, Cr, Ga, Y, Zr, Nb, REE, Hf, Bi, Th and some divalent heavy metals (Ni, Cu, Cd), oxyanions (Sb), Cs, Tl and SO_4. The second group typified highly mobile elements exhibiting lower concentrations during spring flood compared to the baseflow and included DIC, POC, alkaline and alkaline earth metals (Li, Na, Mg, Ca, Sr, Ba), labile nutrients (Si, P, Mn), oxyanions (As, Mo), Fe and U(VI). Finally, a group of elements demonstrated rather similar (within 30%) concentrations during both seasons and included Cl, micronutrients (V, Co, Zn, Se, Rb), Ge, W and Cd.

A pairwise (Pearson) correlation of major and trace element concentration in the main stem and tributaries of the Ket River with main land cover parameters of the watershed was tested for both seasons, but notable correlations were observed only for the summer baseflow (**Table S3**). These correlations were detected only alkaline-earth elements (Mg, Ca, Sr) and U, whose concentrations positively correlated ($R_{Pearson} \geq 0.5$; $p < 0.05$) with phytomass stock on the watersheds (**Fig. 4**). However, these correlations do not necessarily indicate a direct control but may be the consequence of the fact that carbonate-bearing loesses are most favorable substrate for productive forests compared to clay, sand and peat –rich soils [20].

Preprints (www.preprints.org) | NOT PEER-REVIEWED | Posted: 30 June 2022 doi:10.20944/preprints202206.0422.v1

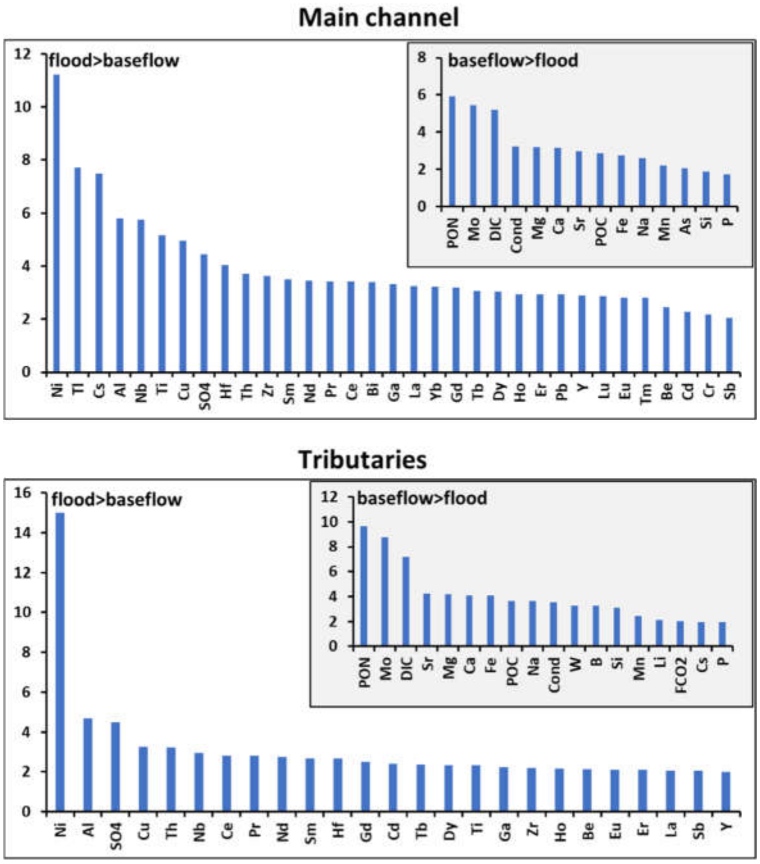

Figure 3. Mean ratio of element concentrations between spring flood period and summer baseflow in the Ket River main stem and tributaries.

The carbonate minerals of these substrates are known to act as sizable sources of alkaline-earth metals and uranium [the latter is carried in the form of highly labile uranyl-carbonate complexes] in shallow subsurface and groundwater feeding the river during summer baseflow [16, 17]. The other elements did not demonstrate any sizable correlations to the landscape factors. The most likely reason for paucity of such a control is highly homogeneous coverage of the river basins by forest, bogs and riparian zones with essentially the same climate, runoff, forest, soil, and total phytomass stock, represented by similar increasing tree species of the boreal taiga of permafrost-free zone of the WSL.

Preprints (www.preprints.org) | NOT PEER-REVIEWED | Posted: 30 June 2022 doi:10.20944/preprints202206.0422.v1

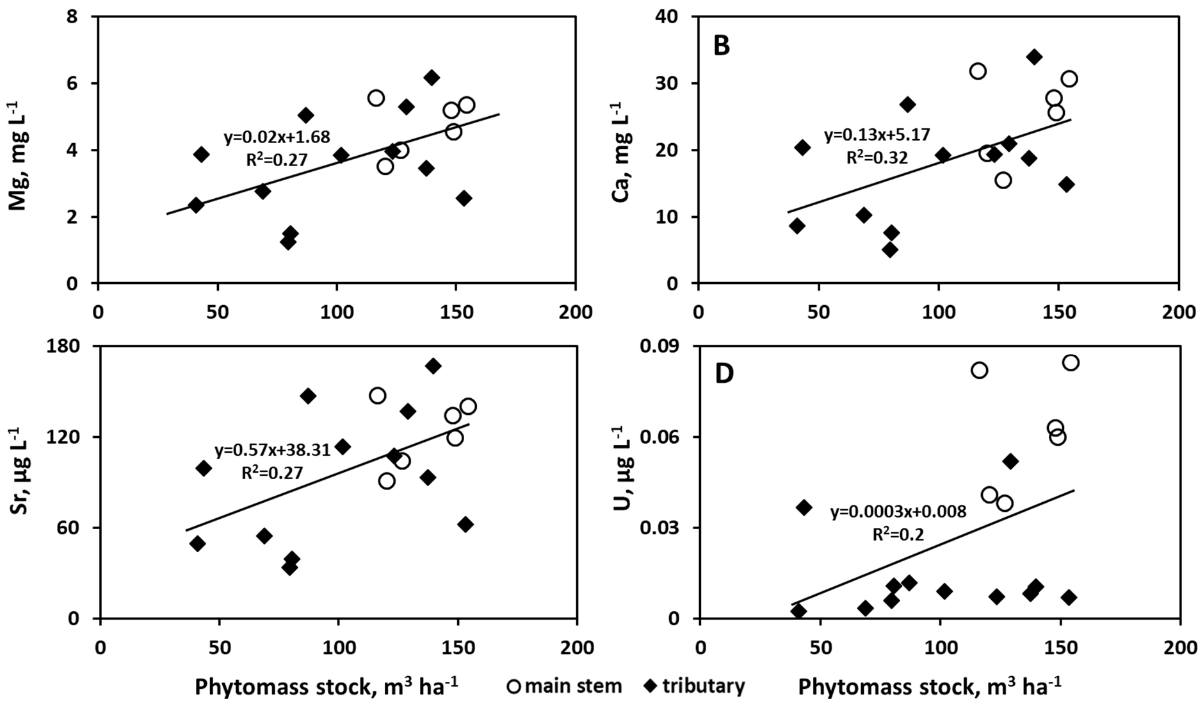

Figure 4. Example of positive correlations between Mg (A), Ca (B), Sr (C) and U (D) and landscape factors of the Ket River in summer.

3.2. Major and trace element spatial variation over the river main stem and among tributaries of the Taz River basin and land cover control

The variations of major and trace element concentration along the Taz River were also rather low as illustrated in a plot of some major and trace element concentrations over the river distance, from the headwaters to the mouth (**Fig. 5**). The concentration of DOC, P_{tot}, NO_3, NO_2, Al, Fe, Cd, Ba and Bi increased southward, with an increase in mean annual temperature. In contrast, in the northward direction, with an increase in tundra and discontinuous permafrost coverage, the concentrations of Cl, SO_4, Li, B, Na, K, V, Ni, Cu, Y, REE and U increased, which may stem from a combination of sea-salts release from the underlying marine clays and silts and far-range (> 300 km) atmospheric transfer from the Norilsk smelters. The variations among tributaries were generally larger but did not any exhibited systematic evolution between the upper and lower reaches of the Taz River basin (**Table S4**). In the main stem and tributaries, the difference in dissolved element concentration between the upper (southern) and lower (northern) part of the river has not exceeded 20-30% which was often within the standard deviation of the mean values. The only exception is Mn those concentrations in the tributaries were two times higher in the south compared to the north.

Pairwise correlations of major and trace element concentration in the Taz River basin with main physico-geographical, geocryological and climatic features of the watershed revealed several potential drivers (**Table S5**). The tundra coverage of the watersheds, corresponding to northward directions and proximity to the sea exhibited strong positive ($R_{Pearson} > 0.60$, $p < 0.01$) correlations with Li, B, Na, K, Cl, SO_4 and U. These elements likely originate from sea salts of the former marine clays dominating the bedrocks of river catchments in the northern part of WSL [17] but also the deposition of marine aerosols in the form of snow [38]. The latter is also known to be enriched in Ni and Cu, reflecting the proximity of the low Taz reaches to the Norilsk Cu-Ni smelters in the northern part of WSL. This can explain positive ($R_{Pearson} > 0.50$, $p < 0.05$) correlations between the tundra coverage and the concentrations of Ni and Cu in the rivers of the Taz basin.

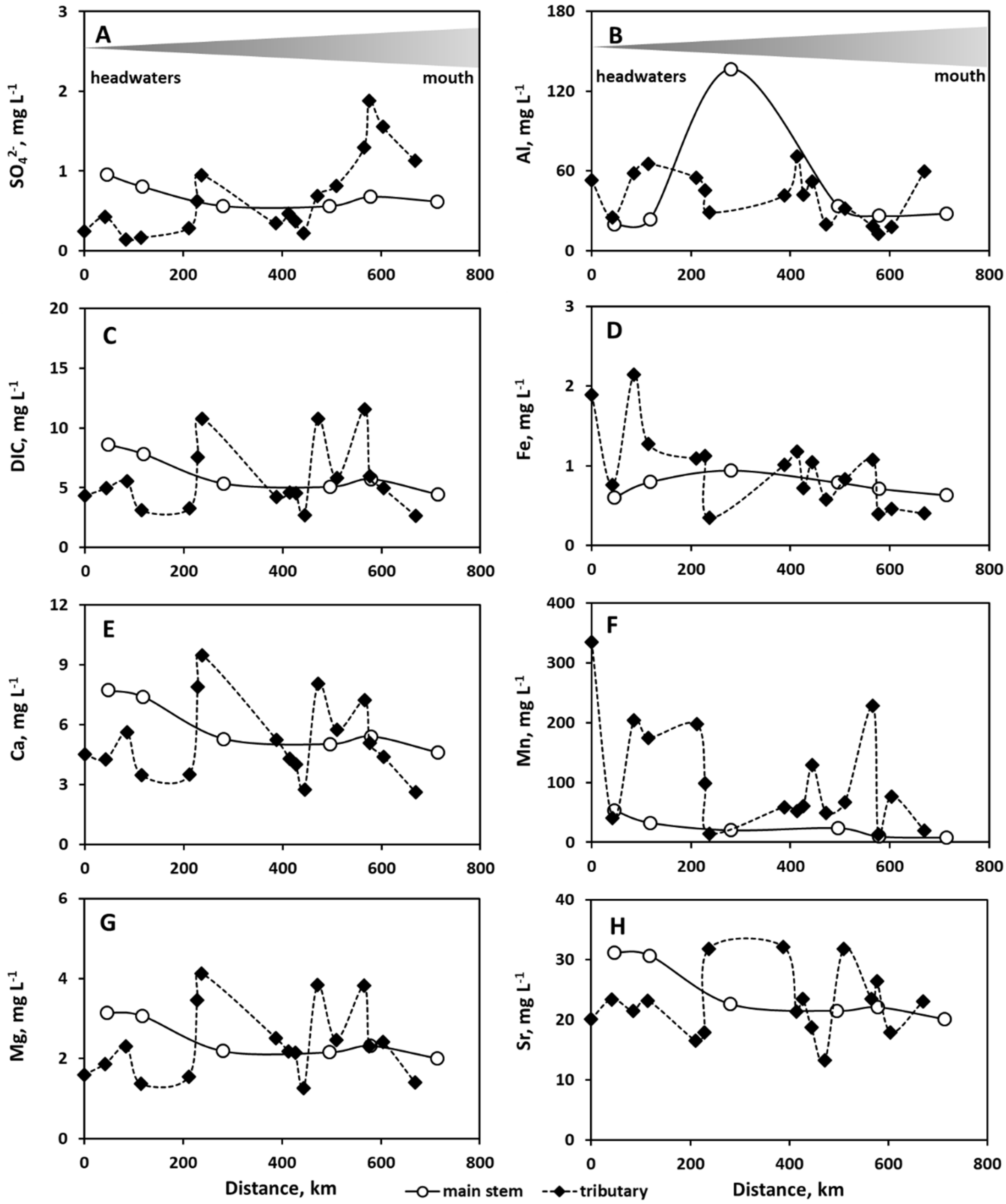

Figure 5. SO_4^{2-} (A), Al (B), DIC (C), Fe (D), Ca (E) Mn (F), Mg (G) and Sr (H) concentration in the Taz River main stem and tributaries during summer baseflow.

The vegetation also exhibited notable impact on elements concentrations in the river water. Thus, presence of larch trees (deciduous needle-leaf forest coverage) positively correlated with concentrations of DOC and macronutrients (Si, Mg, Ca, Sr) and Cs. Light coniferous and broadleaf mixed forest positively impacted concentrations of DOC, macro- (PO_4, NO_3, NH_4) and micro-nutrients (Mn, Fe, Co, Mo, Ba, Cd). Finally, the organic carbon content in upper 0-30 and 0-100 cm of soil positively correlated with some micro-nutrients (Mn, Co, Mo) but also Be, Sc, Cd, Sb and Bi. Noteworthy than neither the watershed surface area nor the permafrost coverage, which are the two potential drivers of element geochemistry in surface waters [i.e., 39-42], correlate with major and trace elements of the Taz River basin. Furthermore, we were not able to detect any control of other landscape features such as riparian zone, wetlands and recent burns.

Preprints (www.preprints.org) | NOT PEER-REVIEWED | Posted: 30 June 2022 doi:10.20944/preprints202206.0422.v1

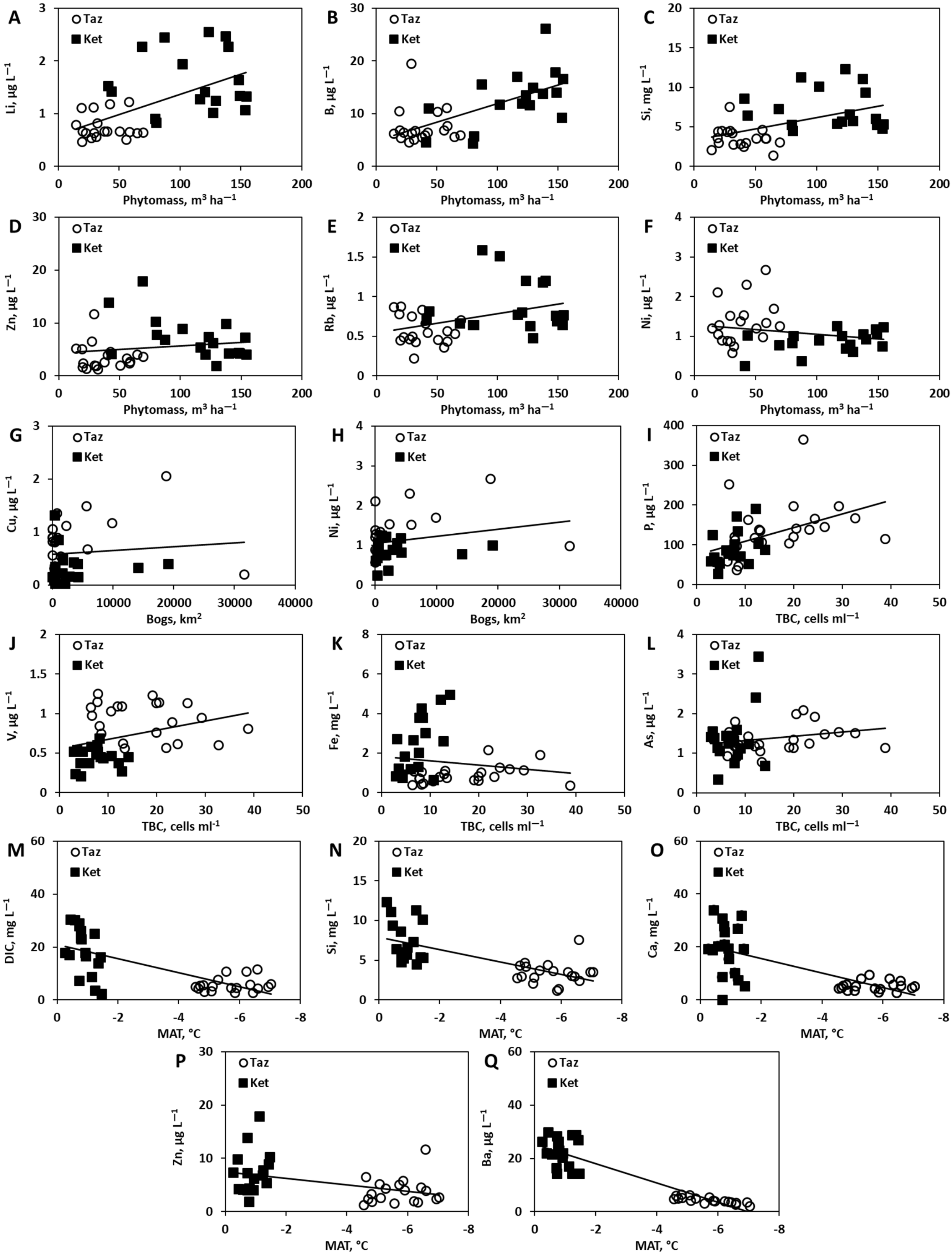

Figure 6. Pairwise correlations of several major and trace elements with two most pronounced landscape parameters - phytomass stock at the watershed and bog coverage, total bacterial count (TBC) and mean air temperature, for both Taz and Ket river main stem and tributaries.

Preprints (www.preprints.org) | NOT PEER-REVIEWED | Posted: 30 June 2022 doi:10.20944/preprints202206.0422.v1

3.3. Common features of spatial distribution of major and trace element in two river basins during summer

The analysis of pairwise correlations described in sections 3.1 and 3.2 for two river basins individually revealed a number of common features in terms of apparent control of landscape parameters on element concentration in river waters. This allowed correlating the hydrochemical composition of the water column with major environmental factors that are likely to operate on both river basins as illustrated for some elements in **Fig. 6**. The first factor is forest biomass in general and in particular, the coverage of the watershed by larch trees (deciduous light needle leaf forest), which are most efficient for recycling the nutrients such as Li, B, Si, Zn, Rb, and Ba [43]. The second environmental parameter is bog coverage of the watershed, positively correlated with SUVA, and low mobile lithogenic elements and divalent transition metals whose transport is facilitated by high DOC concentration (V, Ni, Cu, Y, heavy REE). The impact of bogs on retention of these elements was demonstrated in North European boreal rivers [44, 45].

Noteworthy that the bog presence facilitated only the transport of heavy REE and not the light ones. In the WSL surface waters, the former are known to form much stronger complexes with DOM from bogs and peat waters and less prone to be carried as organo-ferric colloids [30, 46-48]. A small number of elements were associated with total bacterial number (SUVA, P, V, Fe and As) and presumably marked underground discharge of Fe(II) rich waters in the adjacent peatlands and biotically-driven formation of large size Fe hydroxide colloids, stabilized by allochthonous (aromatic) organic carbon. Strong co-precipitation of P, V and As with Fe hydroxides is known from laboratory experiments [49-52] with organic-rich (peatland) waters in the presence of soil and aquatic bacteria. The area of riparian zones of the river positively correlated with DIC, Sr, Ba, U and particulate organic nitrogen. While the first four elements could mark an enhanced discharge of deep and subsurface groundwaters in the riparian zones, notably of larger rivers, the correlation with PON could illustrate the generation of N-rich particles in the sediments of highly productive floodplains [13, 18]. Among common climate parameters of both river basins, the precipitation did not impacted the hydrochemical composition. However, the mean annual air temperature encompassed the contrast between northern and southern rivers and correlated with labile components of the river water (S.C., DIC, Li, B, Si, Ca, Sc, Zn, Se, Rb, Sb, Cs, Ba and U). This was fully consistent with previous observations of large (Ob, ref. 20; Lena, ref. 53) and small [15-17] Siberian rivers.

Given that the season was an important driving factor of element concentrations in the Ket River (see section 3.1), we attempted simultaneous PCA treatment of elementary dataset of both rivers during summer baseflow. This analysis revealed three main factors capable explaining 26, 14 and 6.6 % of total variability, respectively (**Fig. S2, Table S6**). The first factor acted positively on aluminum and other low mobile hydrolysates such as Be, Al, Ti, Cr, Ga, Y, Zr, Nb, Y, REE, Hf, Th and elements which are known to be strongly complexed with DOM such as Cu and Se [54]. Presumably, it reflected mobilization of low soluble elements from lithogenic minerals in the form of organo-mineral (essentially organo-alumunium) colloids as it is known from studies in soil porewaters of the WSL regions [24]. The second factor negatively acted on labile Na, Mg, Si, Ca, P and Fe (probably as Fe(II)). The F2 was also positively linked to DOC, micronutrients (Zn, Rb, Ba) and phytomass at the watershed (primarily, light needle-leaf trees) as well as mean temperature and the proportion of younger (< 25 Ma) rocks. These rocks in the WSL likely contain carbonate concretions and partially carbonated loesses. The second factor thus likely represented a combined effect of productive litter in larch forest growing on carbonate-rich rocks and groundwater feeding of the rivers by soluble, highly mobile elements. Finally, the third factor, although exhibited limited explanation capacity, was strongly linked to pH, specific conductivity, DIC, Sr, and U and clearly marked a direct impact of bicarbonate-rich, slightly mineralized waters that reside in shallow (Taz) and deeper (Ket) subsurface reservoirs containing carbonate minerals, and actively discharge into the river during baseflow.

Noteworthy is the similarity of two main groups of major and trace elements, DOC- and DIC-related, based on pairwise correlations between element concentrations. The DIC concentration in both river basins significantly ($p < 0.05$) correlated with S.C., Si, alkalis (Li, Na), alkaline-earth metals (Mg, Ca, Sr, Ba) and U. This correlation marks an enhanced mobility of these elements in the form of ionic forms and neutral molecules (uranyl as carbonate/hydroxide complexes), essentially controlled by discharge of DIC and mobile element – rich groundwaters either at the river bank or in the hyporheic zone. These mechanisms of labile element mobilization are fairly well known across the boreal zone [55]. The DOC correlated with trivalent (Sc, Al, Ga, Y, REE), tetravalent (Ti, Zr, Hf, Th) and other (Be, Cr, Nb) hydrolysates, Se and Cs. These elements are essentially present in the river water in the form of Al-organic colloids or organic complexes [15, 54, 56-58]. These two main groups of solutes were evidenced not only in large and small rivers and streams [14, 16, 17, 20, 59] but in lentic waters of the region, such as lakes and ponds [60, 61], supra-permafrost waters [23], peat porewaters [22] and peat ice [21].

3.4. Climate change consequences on element concentration in WSL rivers (vegetation and permafrost/lithology control) using a substituting space for time approach

Taking the advantage of highly pristine character of Taz and Ket River basins (in contrast to the neighboring Pur River basin and left tributaries of the Ob River, which are strongly impacted by gas and oil industry), one can use these river systems to approximate future changes in river hydrochemistry linked to on-going climate change and permafrost thaw. For this, we can employ a "substituting space for time" approach which postulates, in a broader context, that spatial phenomena which are observed today can be used to describe past and future events [62]. Such an approach has been successfully used in western Siberia since pioneering work of Frey and Smith [12] to model possible future changes in small rivers [13, 59], lakes [61], soil waters [23] and permafrost ice [21]. Indeed, with permafrost and forest boundary shift northward over next decades [9, 63-65], the northern part of the Taz River (tundra and forest-tundra of continuous to discontinuous permafrost) can be entirely transformed into southern part-like territory of taiga and forest-tundra biome with discontinuous to sporadic permafrost, whereas the entire Ket River basin can be used as a surrogate for hydrochemistry for the southern part of the Taz River. The mean element concentrations in the main stem and tributaries in the two sub-basins of the Taz and Ket River are illustrated in **Fig. 7**. It can be seen that only a few elements exhibited sizable contrast in river water concentration between the southern and northern part of the Taz River basin and the Ket river catchment. Applying a substituting space for time approach, we can anticipate that the concentration of DIC and mobile elements Li, B, Mg, Ca, Sr, Rb, Sb, W, U, and in lesser degree, DOC, Si and micronutrients (Mn, Fe, Zn, Mo) will increase in the low reaches of the Taz River.

Overall, the main consequences of the climate change in western Siberia on middle size river basin hydrochemistry seems to be primarily linked to the changes in dominant vegetation and biomass at the river watershed. In the northern part of the WSL, the change in hydrological pathways due to permafrost thaw might enrich the river waters in soluble elements due to enhanced underground water feeding (DIC, alkaline-earth elements (Ca, Sr), oxyanions (Mo, Sb) and U). The thickening of the active layer may increase the export of trivalent and tetravalent hydrolysates in the form of organo-ferric colloids. However, at the short-term scale, due to two counterbalanced sources and sinks (permafrost thaw and plant uptake), the overall impact of the climate change on inorganic solute export by rivers from the land to the ocean may be smaller than that traditionally viewed for organic carbon.

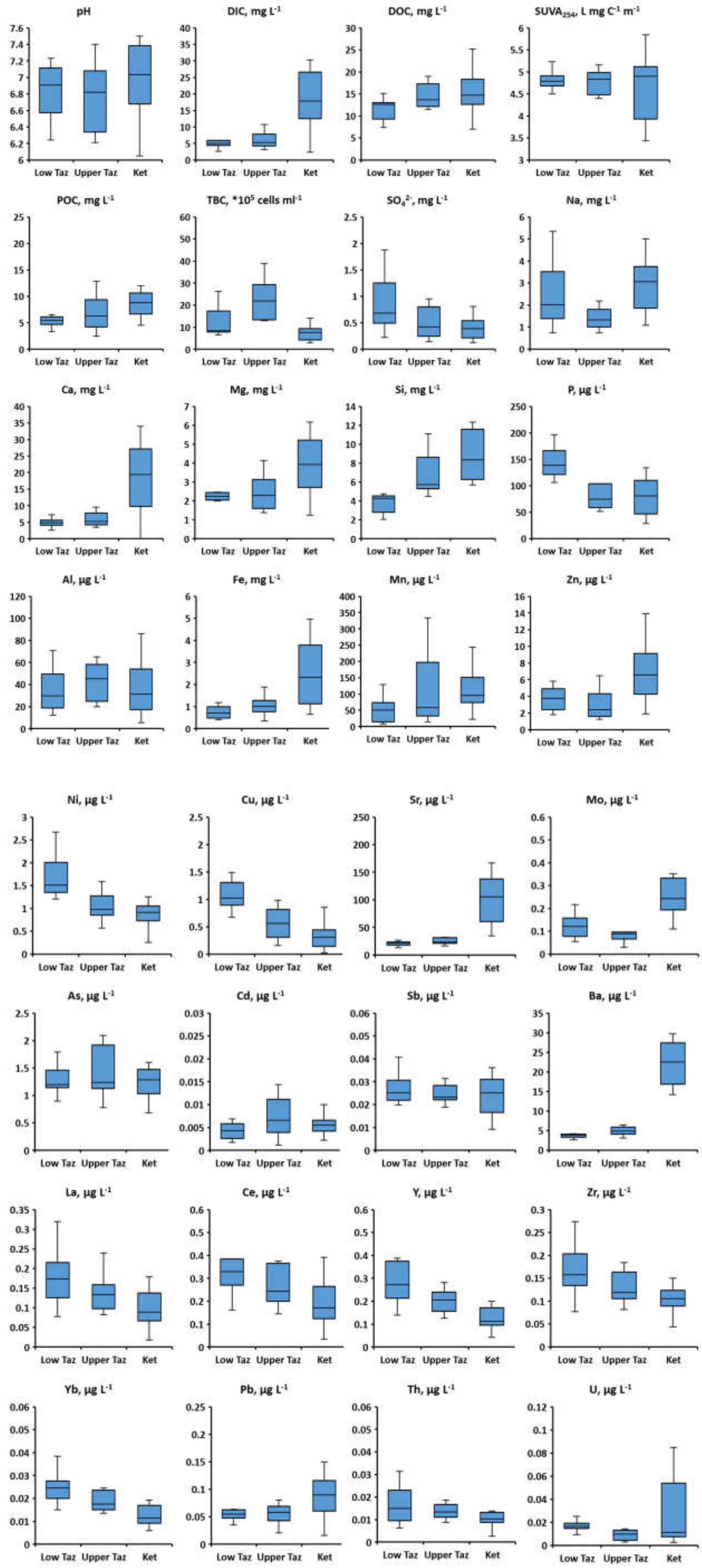

Figure 7. Elements concentration in Upper Taz (0-400 km), Low Taz (400-800 km) and Ket River (main stem and tributaries). Box represents median, whiskers correspond to lower and upper quartile.

5. Conclusions

Towards a better understanding of land cover control on dissolved (< 0.45 µm) major and trace elements in the river water of high latitude regions, we selected two medium-size pristine rivers of the northern, permafrost-bearing and southern, permafrost-free region of the world's largest peatland, the Western Siberia Lowland (Taz and Ket River, respectively). We sampled the main stem and tributaries while encompassing a large gradient in river basin size, permafrost and vegetation coverage at essentially similar lithological substrate, runoff and relief. In the Ket River, the difference in major and trace solute concentration between two seasons was larger than the difference between the main stem and the tributaries. This allowed straightforward comparison of two river basins during the same season (summer baseflow) in order to test the impact of first-order environmental factors on river water hydrochemistry.

The similarity of landscape parameters (mainly, taiga vegetation, partially bogs and permafrost, in less degree the lithology) controlled the major and trace element concentration pattern in two medium-size rivers studied in this work. A number of landscape parameters of the main stem and tributaries watersheds correlated with nutrients (B, Si, Zn, Rb, Ba with phytomass), low mobile lithogenic elements and divalent transition metals whose transport is facilitated by high DOC (V, Ni, Cu, Y, heavy REE with bogs), or specific components reflecting bacterially-controlled DOM processing and groundwater discharge in the water column or within the hyporheic zone (Fe, P, SUVA, V, As). The mean annual air temperature encompassed the contrast between northern and southern rivers and correlated with labile elements of the river water (DIC, Li, B, Si, Ca, Sc, Zn, Se, Rb, Sb, Cs, Ba and U), which was fully consistent with previous observations of large and small Siberian rivers.

Via quantitative comparison of element concentration in south-north gradient of studied river basins, and applying a substituting space for time approach, we infer that permafrost and vegetation shift northward may strongly (a factor of 2 to 3) enrich the river water in the north in highly mobile elements (DIC, Ca, Sr, U), and in a lesser degree, in DOC, POC and nutrients (Si, Mn, Zn, Fe, Mo), whereas the current concentrations of other macro (P) and micro-nutrients (V), and insoluble hydrolysates –geochemical tracers (Y, REE, Zr) in the low reaches of Taz might decrease.

Supplementary Materials: Table S1: Mann-Whitney U Test comparison concentration in different season (flood vs. baseflow) in tributaries and main channel of the Ket River; Table S2: Mean±SD concentrations of elements and other measured parameters in the Ket River main stem and tributaries; Table S3: Table S3. Pairwise Pearson correlations of major and trace element concentrations in the Ket River (main stem and tributaries) during summer baseflow and main hydrochemical parameters of the water column and land cover; Table S4: Hydrochemical parameters of the Taz River basin (stem and tributaries); Table S5: Pearson pairwise correlations of major and trace elements of the river water (Taz and tributaries) with landscape parameters, vegetation coverage and climate; Table S6: Results of PCA of ~65 hydrochemical abd 16 land cover variables in ~ 60 sampling points of the main stem and tributaries of the Ket and Taz River basin, collected during summer baseflow. Fig S1: Seasonal mean±SD concentration elements exhibiting higher concentrations during spring flood compared to summer baseflow in tributaries and main channel Ket' in spring flood (blue) and summer (early fall) baseflow (orange); Fig. S2: Results of PCA of ~65 hydrochemical abd 16 land cover variables in ~ 60 sampling points of the main stem and tributaries of the Ket and Taz River basin, collected during summer baseflow.

Authors' contribution: O.S. Pokrovsky designed the study and wrote the paper; A.G. Lim and I.A. Krickov performed sampling, analysis and their interpretation; S.N. Vorobyev and O.S. Pokrovsky were responsible for the choice of sampling objects and statistical treatment. L.S. Shirokova was in charge of DOC and bacterial analyses and their interpretation; M. Korets provided the GIS data for river watersheds from available databases. Each co-author have seen and approved the final paper and contributed to writing the manuscript.

Acknowledgements: We acknowledge support from RSF grant 22-17-00253, RFBR grant 20-05-00729, the TSU Development Program "Priority-2030", and grant "Kolmogorov" of MES (Agreement No 075-15-2022-241).

Conflicts of Interest: The authors declare no conflict of interest

References

1. Frey, K.E.; McClelland, J. W. Impacts of permafrost degradation on arctic river biogeochemistry. *Hydrol. Process.* **2009,** *23,* 169–182.
2. Vonk, J.E.; Tank, S.E.; Bowden, W.B.; Laurion, I.; Vincent, W.F.; Alekseychik, P.; Amyot, M.; Billet, M.F.; Canário, J.; Cory, R.M.; Deshpande, B.N.; Helbig, M.; Jammet, M.; Karlsson, J.; Larouche, J.; MacMillan, G.; Rautio, M.; Walter Anthony, K.M.; Wickland, K.P. Reviews and Syntheses: Effects of permafrost thaw on arctic aquatic ecosystems. *Biogeosciences* **2015,** *12,* 7129-7167.
3. Vonk, J.E.; Tank, S.E.; Walvoord, M.A. Integrating hydrology and biogeochemistry across frozen landscapes. *Nat. Commun*. **2019**, 10, 1–4. https://doi.org/10.1038/s41467-019-13361-5
4. White, D.; Hinzman, L.; Alessa, L.; Cassano, J.; Chambers, M.; Falkner, K.; Francis, J.; Gutowski Jr.; W.J., Holland, M.; Holmes, R.M.; Huntington, H.; Kane, D.; Kliskey, A.; Lee, C.; McClelland, J.; Peterson, B.; Rupp, T.S.; Straneo, F.; Steele, M.; Woodgate, R.; Yang, D.; Yoshikawa, K.; Zhang T. The arctic freshwater system: Changes and impacts. *J. Geophys. Res.* **2007,** *112*, G04S54, doi:10.1029/2006JG000353.
5. Beilman, D.W.; MacDonald, G.M.; Smith, L.C.; Reimer, P.J. Carbon accumulation in peatlands of West Siberia over the last 2000 years. *Global Biogeochem. Cycles* **2009,** *23,* GB1012, doi:10.1029/2007GB003112.
6. Botch, M.S.; Kobak, K.I.; Vinson, T.S.; Kolchugina, T.P. Carbon pools and accumulation in peatlands of the former Soviet Union. *Global Biogeochem. Cycles* **1995,** *9,* 37–46, doi: 10.1029/94GB03156.
7. Frey, K.E.; Smith, L.C. How well do we know northern land cover? Comparison of four global vegetation and wetland products with a new ground-truth database for West Siberia. *Global Biogeochem. Cycles* **2007,** *21,* GB1016, doi:10.1029/2006GB002706.
8. Kremenetsky, K.V.; Velichko, A.A.; Borisova, O.K.; MacDonald, G.M.; Smith, L.C.; Frey, K.E.; Orlova, L.A.: Peatlands of the West Siberian Lowlands: Current knowledge on zonation, carbon content, and Late Quaternary history. *Quaternary Sci. Rev.* **2003,** *22,* 703–723, 2003.
9. Romanovsky, V.E.; Drozdov, D.S.; Oberman, N.G.; Malkova, G.V.; Kholodov, A.L.; Marchenko, S.S.; Moskalenko, N.G.; Sergeev, D.O.; Ukraintseva, N.G.; Abramov, A.A.; Gilichinsky, D.A., Vasiliev, A.A. Thermal state of permafrost in Russia. *Permafrost Periglacial Proc.* **2010,** *21,* 136–155, doi:10.1002/ppp.683.
10. Smith, L.C.; Macdonald, G.M.; Velichko, A.A.; Beilman, D.W.; Borisova, O.K.; Frey, K.E.; Kremenetsky, K.V.; Sheng, Y. Siberian peatlands as a net carbon sink and global methane source since the early Holocene. *Science* **2004,** *303,* 353–356.
11. Frey, K.E.; Siegel, D.I.; Smith, L.C. Geochemistry of west Siberian streams and their potential response to permafrost degradation. *Water Resour. Res*. **2007b**, *43*, doi:10.1029/2006WR004902.
12. Frey, K.E.; Smith, L.C. Amplified carbon release from vast West Siberian peatlands by 2100. *Geophys. Res. Lett*. **2005**, *32*, doi:10.1029/2004GL022025.
13. Krickov, I., Lim, A., Manasypov, R. M., Loiko, S. V., Shirokova, L. S., Kirpotin, S. N., Karlsson, J. and Pokrovsky, O. S. Riverine particulate C and N generated at the permafrost thaw front: case study of western Siberian rivers across a 1700-km latitudinal transect. *Biogeosciences* **2018**, *15*, 6867–6884. https://doi. org/10.5194/bg-15-6867-20.
14. Krickov, I.V.; Pokrovsky, O.S.; Manasypov, R.M.; Lim, A.G.; Shirokova, L.S.; Viers, J. Colloidal transport of carbon and metals by western Siberian rivers during different seasons across a permafrost gradient. *Geochim. Cosmochim. Acta* **2019**, *265*, 221–241, doi:10.1016/j.gca.2019.08.041.
15. Krickov, I.V.; Lim, A.G.; Manasypov, R.M.; Loiko, S.V.; Vorobyev, S.N.; Shevchenko, V.P.; Dara, O.M.; Gordeev, V.V.; Pokrovsky, O.S. Major and trace elements in suspended matter of western Siberian rivers: First assessment across permafrost zones and landscape parameters of watersheds. *Geochim. Cosmochim. Acta* **2020**, *269*, 429–450, doi:10.1016/j.gca.2019.11.005
16. Pokrovsky, O.S.; Manasypov, R.M.; Shirokova, L.S.; Loiko, S.V.; Krickov, I.V.; Kopysov, S. Zemtzov V.A.; Kulizhsky S.P.; Vorobyev S.N.; Kirpotin S.N. Permafrost coverage, watershed area and season control of dissolved carbon and major elements in western Siberia rivers. *Biogeosciences* **2015**, *12*, 6301–6320.
17. Pokrovsky, O.S.; Manasypov, R.M.; Loiko, S.; Krickov, I.A.; Kopysov, S.G.; Kolesnichenko, L. G.; Vorobyev, S.N.; Kirpotin, S.N. Trace element transport in western Siberia rivers across a permafrost gradient. *Biogeosciences* **2016a**, *13*(6), 1877–1900.
18. Vorobyev, S.N.; Pokrovsky, O.S.; Serikova, S.; Manasypov, R.M.; Krickov, I.V.; Shirokova, L.S.; Lim, A.; Kolesnichenko, L.G.; Kirpotin, S.N.; Karlsson, J. Permafrost boundary shift in Western Siberia may not modify dissolved nutrient concentrations in rivers. *Water* **2017**, *9*, 985, doi:10.3390/w9120985.
19. Vorobyev, S.N.; Pokrovsky, O.S.; Kolesnichenko, L.G.; Manasypov, R.M.; Shirokova, L.S.; Karlsson, J.; Kirpotin, S.N. Biogeochemistry of dissolved carbon, major, and trace elements during spring flood periods on the Ob River. *Hydrological Processes* **2019**, *33*, 1579–1594, doi:10.1002/hyp.13424.
20. Kolesnichenko Y.; Kolesnichenko L.G.; Vorovyev S.N.; Shirokova L.S.; Semiletov I.P.; Dudarev O.V.; Vorobyev R.S.; Shavrina U.; Kirpotin, S.N.; Pokrovsky, O.S. Landscape, soil, lithology, climate and permafrost control on dissolved carbon, major and trace elements in the Ob River, western Siberia. *Water (MDPI)* **2021,** *13,* Art No 3189. https://doi.org/10.3390/w13223189.
21. Lim, A.G.; Loiko, S.V.; Kuzmina, D.; Krickov, I.V.; Shirokova, L.S.; Kulizhsky, S.P.; Vorobyev, S.N.; Pokrovsky, O.S. Dispersed ground ice of permafrost peatlands: a non-accounted for source of C, nutrients and metals. *Chemosphere,* **2021,** *226,* Art No 128953. https://doi.org/10.1016/j.chemosphere.2020.128953.

22. Raudina, T.V.; Loiko, S.V.; Lim, A.G.; Krickov, I.V.; Shirokova, L.S.; Istigichev, G.I.; Kuzmina, D.M.; Kulizhsky, S.P.; Vorobyev, S.N.; Pokrovsky, O.S. Dissolved organic carbon and major and trace elements in peat porewater of sporadic, discontinuous, and continuous permafrost zones of western Siberia. *Biogeosciences* **2017,** *14*(14), 3561–3584, https://doi.org/10.5194/bg-14-3561-2017
23. Raudina, T.V.; Loiko, S.V.; Lim, A.; Manasypov, R.M.; Shirokova, L.S.; Istigechev, G.I.; Kuzmina, D.M.; Kulizhsky, S.P.; Vorobyev, S.N.; Pokrovsky, O.S. Permafrost thaw and climate warming may decrease the CO_2, carbon, and metal concentration in peat soil waters of the Western Siberia Lowland. *Sci. Total Environ.* **2018**, *634*, 1004–1023, doi:10.1016/j.scitotenv.2018.04.059.
24. Raudina, T.V.; Loiko, S.; Kuzmina, D.M.; Shirokova, L.S.; Kulizhsky, S.P.; Golovatskaya, E.A.; Pokrovsky, O.S. Colloidal organic carbon and trace elements in peat porewaters across a permafrost gradient in Western Siberia. *Geoderma* **2021**, *390*, Art No 114971, https://doi.org/10.1016/j.geoderma.2021.114971.
25. Karlsson, J.; Serikova, S.; Vorobyev, S.N.; Rocher-Ros, G.; Denfeld, B.; Pokrovsky, O.S. Carbon emission from Western Siberian inland waters. *Nature Comm.* **2021,** *12*, 825, https://doi.org/10.1038/s41467-021-21054-1.
26. Serikova, S.; Pokrovsky, O.S.; Ala-Aho, P.; Kazantsev, V.; Kirpotin, S.N.; Kopysov, S.G.; Krickov, I.V.; Laudon, H.; Manasypov, R.M.; Shirokova, L.S.; Soulsby, D.T.; Karlsson J. High riverine CO_2 emissions at the permafrost boundary of Western Siberia. *Nature Geoscience* **2018**, *11*, 825–829, doi:10.1038/s41561-018-0218-1
27. Serikova, S.; Pokrovsky, O.S.; Laudon, H.; Krickov, I.V.; Lim, A.G.; Manasypov, R.M.; Karlsson, J. High carbon emissions from thermokarst lakes of Western Siberia. *Nat. Commun*. **2019**, *10*, 1–7, doi:10.1038/s41467-019-09592-129.
28. Pokrovsky, O.; Lim, A.; Korets, M.; Krickov, I.; Vorobyev, S. Dissolved (< 0.45 µm) major and trace elements and landscape parameters of Ket and Taz Rivers, Western Siberia. *Mendeley Data* **2022,** *V1*, doi: 10.17632/rgwzydrg92.1.
29. Marie, D. ; Partensky, F. ; Vaulot, D. ; Brussaard, C. Enumeration of phytoplankton, bacteria, and viruses in marine samples. *Current Protocols Cytometry* **1999,** *10(1)*, 11111–111115. https://doi.org/10.1002/0471142956.cy1111s10.
30. Pokrovsky, O.S.; Manasypov, R.M.; Loiko, S.V.; Shirokova, L.S. Organic and organo-mineral colloids in discontinuous permafrost zone. *Geochim. Cosmochim. Acta* **2016b**, *188*, 1–20, doi:10.1016/j.gca.2016.05.035.
31. Shirokova, L.S.; Pokrovsky, O.S.; Kirpotin, S.N.; Desmukh, C.; Pokrovsky, B.G.; Audry, S.; Viers, J. Biogeochemistry of organic carbon, CO_2, CH_4, and trace elements in thermokarst water bodies in discontinuous permafrost zones of Western Siberia. *Biogeochemistry* **2013,** *113*, 573–593.
32. Heimburger, A.; Tharaud, M.; Monna, F.; Losno, R.; Desboeufs, K.; Nguyen, E.B. SLRS-5 elemental concentrations deduced from SLRS-5/SLRS-4 ratios of thirty-three uncertified elements. *Geostand. Geoanal. Res.* **2013,** *37*, 77–85. https://doi.org/10.1111/J.1751-908X.2012.00185.X
33. Yeghicheyan, D.; Bossy, C.; Bouhnik Le Coz, M.; Douchet, Ch.; Granier, G.; Heimburger, A.; Lacan, F.; Lanzanova, A.; Rousseau, T.C.C.; Seidel, J.-L.; Tharaud, M.; Candaudap, F.; Chmeleff, J.; Cloquet, C.; Delpoux, S.; Labatut, M.; Losno, R.; Pradoux, C.; Sivry, Y.; Sonke, J. E. A Compilation of Silicon, Rare Earth Element and Twenty-One other Trace Element Concentrations in the Natural River Water Reference Material SLRS-5 (NRC-CNRC). *Geostand. Geoanal. Res.* **2013,** *37*, 449–467, doi:10.1111/j.1751-908X.2013.00232.x.
34. Bartalev, S.A.; Egorov, V.A.; Ershov, D.V.; Isaev, A.S.; Lupyan, E.A.; Plotnikov, D.E.; Uvarov, I. A. Remote mapping of vegetation land cover of Russia based on data of MODIS spectroradmeter. *Modern Problems of Earth Remote Sensing from Space*, **2011,** *8(No 4)*, 285-302. http://d33.infospace.ru/d33_conf/2011v8n4/285-302.pdf.
35. Harris, I.; Jones, P. D.; Osborn, T. J.; Lister, D. H. Updated high-resolution grids of monthly climatic observations – the CRU TS3.10 Dataset. *Int. J. Climatol.* **2014,** *34*, 623–642, doi: 10.1002/joc.3711.
36. Hugelius, G.; Tarnocai, C.; Broll, G.; Canadell, J.G.; Kuhry, P.; Swanson, D.K. The Northern Circumpolar Soil Carbon Database: spatially distributed datasets of soil coverage and soil carbon storage in the northern permafrost regions. *Earth Syst. Sci. Data* **2013,** *5*, 3–13, https://doi.org/10.5194/essd-5-3-2013.
37. Santoro, M.; Beer, C.; Cartus, O.; Schmullius, C.; Shvidenko, A.; McCallum, I.; Wegmueller, U.; Wiesmann, A. The BIOMASAR algorithm: An approach for retrieval of forest growing stock volume using stacks of multi-temporal SAR data, 2010 In: Proceedings of ESA Living Planet Symposium, 28 June-2 July 2010 (https://www.researchgate.net/publication/230662433, http://pure.iiasa.ac.at/id/eprint/9430/).
38. Krickov, I.V.; Lim, A.G.; Shevchenko, V.P.; Vorobyev S.N.; Candadaup, F.; Pokrovsky, O.S. Dissolved metal (Fe, Mn, Zn, Ni, Cu, Co, Cd, Pb) and metalloid (As, Sb) in snow water across a 2800-km latitudinal profile of western Siberia: impact of local pollution and global transfer. *Water* **2022,** *14,* Art No 94. https://doi.org/10.3390/w14010094.
39. Barker, A.J.; Douglas, T.A.; Jacobson, A.D.; McClelland, J.W.; Ilgen A.G.; Khosh, M.S.; Lehn, G.O.; Trainor, T.P. Late season mobilization of trace metals in two small Alaskan arctic watersheds as a proxy for landscape scale permafrost active layer dynamics. *Chemical Geology* **2014,** *381*, 180-193.
40. Keller, K.; Blum, J.D.; Kling, G.W. Geochemistry of soils and streams on surfaces of varying ages in arctic Alaska, *Arct. Antarct. Alp. Res.* **2007,** *39*, 84–98.
41. Keller, K.; Blum, J.D.; Kling, G.W. Stream geochemistry as an indicator of increasing permafrost thaw depth in an arctic watershed. *Chem. Geol.* **2010**, *273*, 76–81.
42. Laudon, H.; Sjoblom, V.; Buffam, I.; Seibert, J.; Morth, M. The role of catchment scale and landscape characteristics for runoff generation of boreal streams. *J. Hydrol.* **2007,** *344*, 198-209.

43. Viers, J.; Prokushkin, A.S.; Pokrovsky, O.S.; Beaulieu, E.; Oliva, P.; Dupré B. Seasonal and spatial variability of elemental concentrations in boreal forest larch folliage of Central Siberia on continuous permafrost. *Biogeochemistry* **2013,** *113*, 435-449.
44. Lidman, F.; Morth, C.M.; Laudon, H. Landscape control of uranium and thorium in boreal streams – spatiotemporal variability and the role of wetlands. *Biogeosciences* **2012,** *9*, 4773-4785.
45. Lidman, F.; Kohler, S.J.; Morth, C.-M.; Laudon, H.: Metal transport in the boreal landscape – the role of wetlands and the affinity for organic matter. *Environ. Sci. Technol.* **2014,** *48*, 3783-3790.
46. Ingri, J., Widerlund, A., Land, M., Gustafsson, Ö., Andersson, P.S., and Öhlander, B.: Temporal variations in the fractionation of the rare earth elements in a boreal river, the role of colloidal particles. *Chem. Geol.* **2000,** *166*, 23-45.
47. Stolpe, B.; Guo, L.; Shiller, A.M.; Aiken, G.R. Abundance, size distribution and trace-element binding of organic and iron-rich nanocolloids in Alaskan rivers, as revealed by field-flow fractionation and ICP-MS. *Geochim Cosmochim Acta* **2013,** *105,* 221-239.
48. Vasyukova, E.V.; Pokrovsky, O.S.; Viers, J.; Oliva, P.; Dupré, B.; Martin, F.; Candadaup, F. Trace elements in organic- and iron-rich surficial fluids of the boreal zone: Assessing colloidal forms via dialysis and ultrafiltration. *Geochim. Cosmochim. Acta* **2010,** *74*, 449-468.
49. Oleinikova, O.; Drozdova, O.Y.; Lapitskiy, S.A.; Bychkov, A.Y.; Pokrovsky, O.S. Dissolved organic matter degradation by sunlight coagulates organo-mineral colloids and produces low-molecular weight fraction of metals in boreal humic waters. *Geochim. Cosmochim. Acta* **2017,** *211*, 97–114.
50. Oleinikova, O.; Shirokova, L.S.; Gérard, E.; Drozdova, O.Yu.; Lapitsky, S.A.; Bychkov, A.Y.; Pokrovsky, O.S. Transformation of organo-ferric peat colloids by a heterotrophic bacterium. *Geochim Cosmochim Acta* **2017,** *205*, 313–330.
51. Shirokova, L.S.; Bredoire, R.; Rolls, J.-L.; Pokrovsky, O.S. Moss and peat leachate degradability by heterotrophic bacteria: fate of organic carbon and trace metals. *Geomicrobiol. J.* **2017,** *34(8)*, 641-655.
52. Shirokova, L.S.; Chupakova, A.A.; Chupakov, A.V.; Pokrovsky, O.S. Transformation of dissolved organic matter and related trace element in the mouth zone of the largest European Arctic river: experimental modeling. *Inland Waters* **2017,** *7(3),* 272-282.
53. Vorovyev, S.N.; Kolesnichenko, Y.; Korets, M.; Pokrovsky, O.S. Testing landscape, climate and lithology impact on hydrochemical features of the Lena River and its tributaries. *Water (MDPI)* **2021,** *13,* Art No 2093. https://doi.org/10.3390/w13152093.
54. Pokrovsky, O.S.; Bueno, M.; Manasypov, R.M.; Shirokova, L.S.; Karlsson, J.; Amouroux D. Dissolved organic matter controls on seasonal and spatial selenium concentration variability in thaw lakes across a permafrost gradient. *Environmental Science Technology* **2018,** *52 (18),* 10254–10262, DOI: 10.1021/acs.est.8b00918.
55. Chupakov, A.V.; Pokrovsky, O.S.; Moreva, O.Y.; Shirokova, L.S.; Neverova, N.V.; Chupakova, A.A.; Kotova, E.I.; Vorobyeva, T.Y. High resolution multi-annual riverine fluxes of organic carbon, nutrient and trace element from the largest European Arctic river, Severnaya Dvina. *Chemical Geology* **2020,** *538,* doi:10.1016/j.chemgeo.2020.119491.
56. Bagard, M.L.; Chabaux, F.; Pokrovsky, O.S.; Prokushkin, A.S.; Viers, J.; Dupré, B.; Stille, P. Seasonal variability of element fluxes in two Central Siberian rivers draining high latitude permafrost dominated areas. *Geochim. Cosmochim. Acta* **2011,** 75, 3335–3357.
57. Dahlqvist, R.; Andersson, K.; Ingri, J.; Larsson, T.; Stolpe, B.; Turner, D.: Temporal variations of colloidal carrier phases and associated trace elements in a boreal river. *Geochim. Cosmochim. Acta* **2007,** *71,* 5339-5354.
58. Lyvén, B.; Hassellöv, M.; Turner, D.R.; Haraldsson, C.; Andersson, K. Competition between iron- and carbon-based colloidal carriers for trace metals in a freshwater assessed using flow field-flow fractionation coupled to ICPMS. *Geochim. Cosmochim. Acta* **2003,** *67,* 3791-3802.
59. Pokrovsky, O.S.; Manasypov, R.M.; Kopysov, S.; Krickov, I.V.; Shirokova, L.S.; Loiko, S.V.; Lim, A.G.; Kolesnichenko, L.G.; Vorobyev, S.N.; Kirpotin, S.N. Impact of permafrost thaw and climate warming on riverine export fluxes of carbon, nutrients and metals in western Siberia. *Water* **2020,** *12,* Art No 1817; doi:10.3390/w12061817.
60. Manasypov, R.M.; Vorobyev, S.N.; Loiko, S.V.; Kritzkov, I.V.; Shirokova, L.S.; Shevchenko, V.P.; Kirpotin, S.N.; Kulizhsky, S.P.; Kolesnichenko, L.G.; Zemtzov, V.A.; Sinkinov, V.V.; Pokrovsky, O.S. Seasonal dynamics of organic carbon and metals in thermokarst lakes from the discontinuous permafrost zone of western Siberia. *Biogeosciences* **2015,** *12*, 3009–3028.
61. Manasypov, R.M.; Lim, A.G.; Krickov, I.V.; Shirokova, L.S.; Vorobyev, S.N.; Kirpotin, S.N.; Pokrovsky, O.S. Spatial and seasonal variations of C, nutrient, and metal concentration in thermokarst lakes of Western Siberia across a permafrost gradient. *Water* **2020,** *12*, 1830. https://doi.org/10.3390/w12061830.
62. Blois, J.L.; Williams, J.W.; Fitzpatrick, M.C.; Jackson, S.T.; Ferrier, S. Space can substitute for time in predicting climate-change effects on biodiversity. *PNAS* **2013**, *110*, 9374–9379, doi:10.1073/pnas.1220228110.
63. García Criado, M.; Myers-Smith, I.H.; Bjorkman, A.D.; Lehmann, C.E.R.; Stevens, N. Woody plant encroachment intensifies under climate change across tundra and savanna biomes, ed M Josée Fortin. *Glob. Ecol. Biogeogr.* **2020,** *29*, 925–943.
64. Mauclet, E.; Agnan, Y.; Hirst, C.; Monhonval, A.; Pereira, B.; Vandeuren, A.; Villani, M.; Ledman, J.; Taylor, M.; Jasinski, B.L.; Schuur, E.A.G.; Opfergelt, S. Changing sub-Arctic tundra vegetation upon permafrost degradation: impact on foliar mineral element cycling. *Biogeosciences* **2022,** *19,* 2333–2351, https://doi.org/10.5194/bg-19-2333-2022.
65. Tape, K.; Sturm, M.; Racine, C. The evidence for shrub expansion in Northern Alaska and the Pan-Arctic. *Glob. Change Biol.* **2006,** *12,* 686–702, doi:10.1111/j.1365-2486.2006.01128.x.

 doi:10.20944/preprints202206.0422.v1

SUPPLEMENTARY MATERIAL

Table S1 A. Mann-Whitney U Test comparison concentration in different season (flood vs. baseflow) in tributaries and main channel of the Ket River.

	tributaries			main channel					tributaries			main channel		
variable	U	Z	p-value	U	Z	p-value		variable	U	Z	p-value	U	Z	p-value
T_{water}	5	-4.7	<0.001	0	-2.9	0.003		Cr	82	2.3	0.021	1	2.8	0.005
pCO_2	61	-2.7	0.007	-	-	-		Mn	44	-3.5	<0.001	6	-2.1	0.038
FCO_2	52	-2.2	0.025	-	-	-		Fe	25	-4.1	<0.001	1	-2.8	0.005
PON	0	-4.9	<0.001	0	-2.9	0.003		Ni	54	3.2	0.001	1	2.8	0.005
POC	4	-4.8	<0.001	0	-2.9	0.003		Cu	33	3.8	<0.001	0	2.9	0.003
TBC	76	-2.5	0.013	-	-	-		Ga	33	3.8	<0.001	1	2.8	0.005
pH	73	-2.6	0.009	4	-2.4	0.018		As	72	-2.6	0.009	0	-2.9	0.003
S.C.	13	-4.5	<0.001	0	-2.9	0.003		Se	81	2.3	0.019	6	2.1	0.038
$SUVA_{254}$	61	-3.0	0.003	-	-	-		Sr	7	-4.7	<0.001	1	-2.8	0.005
Aromaticity	-	-	-	4	2.4	0.018		Y	50	3.3	0.001	0	2.9	0.003
Humification	4	4.8	<0.001	4	2.4	0.018		Zr	54	3.2	0.001	0	2.9	0.003
Cl	60	-3.0	0.003	19	0.2	0.830		Nb	38	3.7	<0.001	0	2.9	0.003
SO_4	26	4.1	<0.001	0	2.9	0.003		Mo	0	-4.9	<0.001	0	-2.9	0.003
DIC	14	-4.4	<0.001	0	-2.9	0.003		Cd	31	3.9	<0.001	0	2.9	0.003
DOC	76	2.5	0.013	2	2.6	0.008		Sb	13	4.5	<0.001	0	2.9	0.003
Li	24	-4.1	<0.001	-	-	-		Cs	-	-	-	0	2.9	0.003
Be	44	3.5	<0.001	0	2.9	0.003		Ba	51	-3.3	0.001	4	-2.4	0.018
B	58	-3.1	0.002	1	-2.8	0.005		La	54	3.2	0.001	0	2.9	0.003
Na	6	-4.7	<0.001	1	-2.8	0.005		Ce	32	3.9	<0.001	0	2.9	0.003
Mg	6	-4.7	<0.001	1	-2.8	0.005		Pr	29	4.0	<0.001	0	2.9	0.003
Al	10	4.6	<0.001	1	2.8	0.005		Nd	31	3.9	<0.001	0	2.9	0.003
Si	0	-4.9	<0.001	0	-2.9	0.003		Sm	29	4.0	<0.001	0	2.9	0.003
P	47	-3.4	0.001	3	-2.5	0.012		Eu	34	3.8	<0.001	0	2.9	0.003
Ca	15	-4.4	<0.001	2	-2.6	0.008		Gd	34	3.8	<0.001	0	2.9	0.003
Sc	38	-3.7	<0.001	-	-	-		Tb	36	3.8	<0.001	0	2.9	0.003
Ti	52	3.3	0.001	0	2.9	0.003		Dy	37	3.7	<0.001	0	2.9	0.003
								Yb	59	3.0	0.002	0	2.9	0.003
								Lu	65	2.8	0.004	0	2.9	0.003
								Hf	39	3.7	<0.001	0	2.9	0.003
								W	81	-2.3	0.019	-	-	-
								Pb	-	-	-	1	2.8	0.005
								Th	23	4.2	<0.001	0	2.9	0.003

Table S1 B. Mann-Whitney U Test comparison concentration tributaries and main channel in different seasons.

Flood			
variable	U	Z	p-value
pCO_2	26	2.9	0.004
PON	16	-3.3	0.001
POC	26	-2.8	0.005
Cl	32	-2.6	0.010
SO_4	38	-2.3	0.021
B	44	-2.0	0.041
Cu	31	-2.6	0.009
Mo	41	-2.2	0.029
Cs	41	-2.2	0.029
W	39	-2.3	0.023

Pb	43	-2.1	0.036
U	30	-2.7	0.008

Baseflow variable	**U**	**Z**	**p-value**
T_{water}	7	-2.7	0.008
pCO_2	5	2.8	0.006
TBC	10	2.4	0.017
pH	13	-2.2	0.031
$SUVA_{254}$	14	2.0	0.044
Humification	10	-2.4	0.017
SO_4	6	-2.8	0.006
Cs	11	2.3	0.022

Table S2. Mean±SD concentrations of elements and other measured parameters in the Ket River main stem and tributaries.

	Tributaries		Main channel	
Variable	Flood	Base flow	Flood	Base flow
Temp.water, °C	9.27±2.11	14.9±1.24	9.93±2.27	16.5±0.54
pH	6.21±0.41	6.71±0.57	6.6±0.46	7.29±0.26
S.C., µS/cm	36.2±15.3	127±62.1	56.3±32.6	181±36.8
Dissolved O_2, mg/L	8.35±1.12	8.02±1.13	9.47±1.07	8.78±0.18
PON, mg/L	0.07±0.04	0.64±0.27	0.16±0.06	0.96±0.22
POC, mg/L	2.2±1.18	8±2.36	3.29±0.47	9.49±1.98
DIC, mg/L	2.31±1.46	16.6±9.83	4.43±4.23	23±5.03
DOC, mg/L	22±4.04	16.5±7.35	20.7±3.62	15±1.35
TBC *10^5 cells/ml	5.72±3.2	8.69±3.21	6.56±3.06	4.94±2.15
$SUVA_{254}$, L/mg C/m	4.38±0.31	4.9±0.66	4.16±0.25	4.26±0.52
Cl, mg/L	0.09±0.06	0.16±0.07	0.16±0.06	0.17±0.01
SO_4, mg/L	1.39±1.13	0.31±0.14	2.59±1.3	0.58±0.18
Li, µg/L	0.84±0.23	1.76±0.63	1.05±0.34	1.3±0.23
Be, µg/L	0.03±0.01	0.01±0.01	0.03±0.01	0.01±0.00
B, µg/L	6.21±1.95	20.2±27.0	7.98±1.79	13.6±3.24
Na, mg/L	0.82±0.25	2.96±1.26	1.12±0.47	2.92±0.81
Mg, mg/L	0.9±0.35	3.76±1.59	1.31±0.71	4.19±1.06
Al, mg/L	197±91	41.8±32.7	187±88	32±16
Si, mg/L	2.60±0.62	8.13±2.7	2.99±0.31	5.61±0.65
P, µg/L	50±13	96.8±48.1	45±14	77±26
Ca, mg/L	4.57±2.4	18.6±9.36	7.06±4.15	22.4±6.66
Sc, µg/L	0.05±0.02	0.1±0.05	0.06±0.02	0.09±0.03
Ti, µg/L	1.9±1.21	0.81±0.43	3.31±2.36	0.64±0.11
V, µg/L	0.53±0.26	0.43±0.13	0.66±0.26	0.49±0.13
Cr, µg/L	0.5±0.19	0.36±0.12	0.57±0.19	0.26±0.04
Mn, µg/L	51.3±27.8	127±66.1	37.2±8.23	82.9±33.71
Fe, mg/L	0.68±0.2	2.78±1.57	0.6±0.25	1.66±0.67
Co, µg/L	0.22±0.11	0.21±0.1	0.22±0.06	0.17±0.08
Ni, µg/L	12.1±28.3	0.81±0.29	11.2±20.8	1±0.20
Cu, µg/L	1.09±0.61	0.33±0.39	1.89±0.77	0.38±0.10
Zn, µg/L	9.4±5.54	8.22±4.44	6.56±2.11	5.04±1.37
Ga, µg/L	0.05±0.02	0.02±0.01	0.07±0.03	0.02±0.00
Ge, µg/L	0.06±0.02	0.05±0.02	0.06±0.02	0.04±0.01
As, µg/L	0.81±0.31	1.37±0.83	0.66±0.13	1.36±0.17
Se, µg/L	0.05±0.02	0.04±0.01	0.07±0.02	0.05±0.01
Rb, µg/L	0.95±0.43	0.95±0.37	0.7±0.12	0.72±0.07
Sr, µg/L	23.3±9.4	99.1±45.9	36.2±19.8	108±29.0
Y, µg/L	0.28±0.13	0.14±0.09	0.37±0.11	0.13±0.04
Zr, µg/L	0.25±0.16	0.11±0.05	0.36±0.18	0.1±0.01
Nb, µg/L	0.01±0.01	0.003±0.002	0.01±0.01	0.003±0.00
Mo, µg/L	0.03±0.02	0.27±0.12	0.05±0.02	0.27±0.15
Cd, µg/L	0.01±0.01	0.01±0.002	0.01±0.004	0.005±0.001
Sb, µg/L	0.05±0.01	0.02±0.01	0.05±0.01	0.03±0.005
Cs, µg/L	0.004±0.003	0.01±0.02	0.01±0.01	0.001±0.0006
Ba, µg/L	15.6±3.85	22.7±5.92	15.8±3.23	22.1±4.76
La, µg/L	0.23±0.1	0.11±0.08	0.30±0.09	0.09±0.02
Ce, µg/L	0.53±0.21	0.19±0.11	0.62±0.18	0.18±0.06
Pr, µg/L	0.07±0.03	0.02±0.01	0.08±0.03	0.02±0.01
Nd, µg/L	0.25±0.11	0.09±0.05	0.31±0.1	0.09±0.03

Sm, µg/L	0.06±0.03	0.02±0.01	0.08±0.02	0.02±0.01
Eu, µg/L	0.01±0.01	0.01±0.003	0.02±0.01	0.007±0.001
Gd, µg/L	0.06±0.03	0.02±0.01	0.08±0.02	0.02±0.01
Tb, µg/L	0.01±0.004	0.004±0.002	0.01±0.003	0.004±0.001
Dy, µg/L	0.05±0.02	0.02±0.01	0.07±0.02	0.02±0.01
Ho, µg/L	0.01±0.005	0.005±0.003	0.01±0.004	0.005±0.001
Er, µg/L	0.03±0.01	0.01±0.01	0.04±0.01	0.01±0.004
Tm, µg/L	0.004±0.002	0.002±0.001	0.01±0.002	0.002±0.001
Yb, µg/L	0.03±0.01	0.01±0.01	0.04±0.01	0.01±0.003
Lu, µg/L	0.004±0.002	0.002±0.001	0.01±0.002	0.002±0.001
Hf, µg/L	0.01±0.01	0.004±0.002	0.01±0.01	0.003±0.0003
W, µg/L	0.002±0.001	0.01±0.01	0.003±0.001	0.003±0.001
Tl, µg/L	0.003±0.001	0.003±0.002	0.02±0.03	0.002±0.001
Pb, µg/L	0.19±0.26	0.1±0.06	0.23±0.12	0.08±0.02
Bi, µg/L	0.02±0.03	0.01±0.02	0.05±0.06	0.01±0.02
Th, µg/L	0.04±0.02	0.01±0.01	0.04±0.02	0.01±0.001
U, µg/L	0.02±0.01	0.02±0.02	0.03±0.02	0.05±0.03

Preprints (www.preprints.org) | NOT PEER-REVIEWED | Posted: 30 June 2022 doi:10.20944/preprints202206.0422.v1

baseflow	Li	Be	B	Na	Mg	Al	Si	P	Ca	Sc	Ti	V	Cr	Mn	Fe	Co	Ni	Cu	Zn	Ga	Ge	As	Se	Rb	Sr	Y	Zr	Nb	Mo	Rh	Cd	Sb	Cs	Ba	La	Ce	Pr	Yb	Hf	W	Tl	Pb	Bi	Th	U
MAAT	0,5	0,1	0,1	0,4	0,2	-0,3	0,3	0,2	0,2	0,1	-0,2	0,3	0,0	0,6	0,1	0,4	0,0	-0,3	-0,2	-0,3	0,0	0,1	-0,2	0,3	0,1	-0,2	-0,3	-0,1	-0,2	0,2	-0,2	-0,3	0,2	0,1	-0,3	-0,3	-0,2	-0,1	-0,4	0,4	0,1	-0,2	0,1	-0,1	-0,1
MAP	0,1	0,1	-0,2	-0,3	-0,4	0,3	0,2	0,3	-0,5	0,2	0,5	-0,3	0,6	0,0	0,4	0,0	-0,3	-0,1	0,7	0,4	0,5	-0,1	-0,2	0,0	-0,3	0,3	0,6	0,3	0,1	-0,2	0,5	0,0	0,4	-0,1	0,4	0,3	0,3	0,4	0,3	0,0	0,2	0,5	0,1	0,3	-0,5
T_{water}	-0,4	0,0	0,0	-0,2	0,0	0,1	-0,5	0,1	0,0	-0,4	0,0	0,4	-0,3	-0,3	-0,1	0,0	0,4	0,5	-0,5	0,2	-0,1	0,6	0,4	-0,5	-0,1	0,2	0,1	0,1	-0,4	0,0	-0,2	0,6	-0,6	-0,3	0,1	0,1	0,1	0,0	0,3	-0,1	-0,3	-0,1	0,1	0,2	0,4
TBC	-0,1	0,0	-0,3	-0,4	-0,5	0,4	0,1	0,4	-0,6	-0,1	0,6	-0,1	0,6	0,0	0,6	-0,1	-0,2	0,1	0,7	0,4	0,6	0,0	-0,2	-0,2	-0,5	0,4	0,7	0,4	0,0	-0,1	0,6	0,1	0,3	-0,3	0,5	0,4	0,4	0,4	0,3	0,2	-0,1	0,7	0,0	0,3	-0,5
Cl^-	0,6	0,1	0,2	0,7	0,4	-0,3	0,4	-0,1	0,5	0,3	-0,4	0,2	-0,4	0,4	-0,2	0,5	0,1	-0,3	-0,4	-0,2	-0,2	-0,2	-0,3	0,7	0,5	-0,2	-0,6	-0,2	-0,3	0,1	-0,4	-0,6	0,0	0,4	-0,3	-0,2	-0,1	-0,2	-0,5	-0,1	0,2	-0,4	-0,3	-0,1	0,2
SO_4^{2-}	0,0	0,1	0,2	0,3	0,3	-0,2	-0,2	0,0	0,4	0,0	-0,3	0,3	-0,5	0,2	-0,3	0,2	0,2	-0,1	-0,6	-0,3	-0,3	0,3	0,2	-0,1	0,3	-0,2	-0,5	-0,1	-0,3	0,1	-0,5	-0,1	-0,4	0,1	-0,3	-0,3	-0,3	-0,3	-0,2	0,0	0,0	-0,4	0,2	-0,1	0,4
DIC	0,2	-0,1	0,4	0,5	0,6	-0,5	0,1	-0,3	0,7	0,1	-0,6	0,1	-0,6	0,3	-0,5	0,2	0,1	-0,2	-0,7	-0,4	-0,6	0,0	0,0	0,3	0,6	-0,5	-0,8	-0,4	-0,1	0,2	-0,6	-0,3	-0,2	0,4	-0,5	-0,5	-0,5	-0,5	-0,6	-0,1	0,0	-0,7	-0,2	-0,4	0,4
DOC	-0,6	0,0	-0,3	-0,7	-0,4	0,4	-0,6	0,1	-0,4	-0,4	0,4	0,0	0,3	-0,4	0,2	-0,3	0,2	0,6	0,2	0,4	0,3	0,3	0,4	-0,7	-0,5	0,3	0,7	0,3	0,2	0,0	0,4	0,7	-0,3	-0,5	0,5	0,4	0,4	0,3	0,5	0,1	-0,3	0,5	0,2	0,2	0,0
SUVA254	0,2	0,2	-0,3	-0,2	-0,5	0,5	0,3	0,6	-0,6	0,1	0,7	0,2	0,6	-0,1	0,7	0,0	-0,1	0,1	0,7	0,5	0,7	0,0	-0,2	0,0	-0,5	0,6	0,7	0,5	-0,3	-0,3	0,4	0,0	0,3	-0,3	0,7	0,7	0,6	0,7	0,5	0,0	0,1	0,7	0,0	0,6	-0,5
Watershed area	0,1	0,3	-0,3	-0,3	-0,5	0,2	0,2	0,1	-0,5	0,1	0,4	-0,2	0,3	-0,4	0,4	-0,5	-0,3	-0,3	0,5	0,3	0,5	-0,3	-0,4	0,2	-0,4	0,4	0,1	0,2	0,1	0,0	-0,1	-0,3	0,2	-0,3	0,4	0,4	0,3	0,4	0,2	-0,1	0,5	0,2	-0,2	0,4	-0,6
Dark Needleleaf Forest	-0,1	0,2	0,1	0,1	0,2	0,0	-0,2	-0,4	0,2	0,2	-0,3	0,4	-0,3	-0,4	-0,3	-0,3	0,4	0,2	-0,3	0,0	-0,2	-0,1	0,3	0,0	0,2	0,1	-0,3	-0,2	0,0	-0,2	-0,3	0,1	-0,5	0,1	0,0	0,1	0,0	-0,1	0,1	-0,2	0,1	-0,3	-0,1	0,0	0,4
Light Needleleaf Forest	-0,2	0,2	0,1	0,0	0,1	0,1	-0,3	-0,4	0,1	0,1	-0,1	0,3	-0,2	-0,6	-0,2	-0,4	0,4	0,3	-0,2	0,1	-0,1	0,0	0,4	-0,1	0,1	0,2	-0,1	-0,2	0,1	0,0	-0,1	0,2	-0,5	0,0	0,1	0,2	0,1	0,0	0,3	-0,1	0,1	-0,2	-0,1	0,0	0,4
Broadleaf Forest	-0,1	0,2	0,1	0,0	0,1	0,1	-0,2	-0,3	0,1	0,1	-0,1	0,3	-0,2	-0,5	-0,2	-0,4	0,3	0,3	-0,2	0,1	-0,1	-0,1	0,3	0,0	0,1	0,2	-0,1	-0,2	0,0	-0,1	-0,1	0,2	-0,4	0,0	0,1	0,1	0,1	0,0	0,2	-0,1	0,1	-0,1	-0,1	0,0	0,3
Mixed Forest	-0,1	0,3	0,1	0,1	0,2	0,0	-0,1	-0,3	0,2	0,2	-0,2	0,5	-0,3	-0,4	-0,2	-0,2	0,4	0,2	-0,3	0,1	-0,1	0,0	0,3	0,0	0,2	0,2	-0,2	-0,1	-0,1	0,0	-0,3	0,0	-0,4	0,1	0,0	0,1	0,1	0,0	0,2	-0,1	0,2	-0,3	0,1	0,1	0,4
Peatlands and bogs	-0,2	0,2	0,0	-0,2	0,0	0,0	-0,2	-0,4	0,0	0,1	-0,1	0,3	-0,1	-0,7	-0,1	-0,6	0,3	0,3	-0,1	0,3	-0,1	-0,2	0,3	0,0	0,0	0,4	0,1	-0,2	0,1	0,1	-0,1	0,2	-0,4	-0,1	0,3	0,3	0,2	0,2	0,4	-0,2	0,3	-0,1	-0,2	0,1	0,2
Riparian Vegetation	-0,1	0,0	0,0	-0,2	-0,1	0,0	-0,2	0,0	-0,1	-0,2	0,0	0,6	-0,1	-0,4	0,2	-0,3	0,2	0,3	-0,2	0,2	0,1	0,1	0,1	-0,2	-0,2	0,3	0,1	-0,1	-0,3	-0,2	-0,2	0,2	-0,5	-0,3	0,2	0,2	0,1	0,2	0,3	0,0	0,0	0,0	-0,2	0,1	0,2
Grassland	-0,1	0,1	0,2	0,1	0,3	-0,1	-0,2	-0,5	0,4	0,1	-0,3	0,5	-0,4	-0,4	-0,4	-0,3	0,5	0,3	-0,4	0,0	-0,3	-0,1	0,3	0,1	0,3	0,1	-0,3	-0,3	0,0	-0,2	-0,2	0,1	-0,5	0,2	0,0	0,0	0,0	-0,1	0,1	-0,2	0,0	-0,3	-0,1	-0,1	0,5
Recent Burns	-0,1	0,4	0,1	0,0	0,1	0,1	-0,1	-0,2	0,1	0,2	-0,1	0,4	0,0	-0,5	-0,1	-0,3	0,3	0,2	-0,1	0,2	0,0	-0,1	0,3	0,0	0,0	0,3	0,0	-0,1	-0,1	0,1	-0,1	0,1	-0,3	0,0	0,2	0,2	0,2	0,2	0,3	0,0	0,3	-0,1	0,1	0,2	0,2
Water Bodies	-0,1	0,1	-0,2	-0,3	-0,2	-0,1	0,0	-0,4	-0,2	0,0	0,0	0,2	0,0	-0,8	0,1	-0,7	0,0	0,1	0,1	0,2	0,0	-0,4	0,0	0,0	-0,2	0,4	0,2	-0,1	0,0	-0,1	-0,2	0,0	-0,3	-0,2	0,3	0,3	0,3	0,3	0,3	-0,3	0,2	0,0	-0,4	0,0	0,1
Phytomass	0,0	0,2	0,4	0,5	0,5	0,0	-0,2	-0,1	0,50	0,2	-0,4	0,2	-0,4	0,2	-0,5	0,4	0,4	0,1	-0,5	-0,3	-0,4	0,3	0,4	0,0	0,5	-0,3	-0,5	-0,2	-0,1	0,2	-0,2	0,1	-0,3	0,3	-0,4	-0,3	-0,3	-0,4	-0,2	0,1	-0,1	-0,4	0,4	-0,1	0,5
Upper Cretac, Maastrichtian - Lower Paleoc	-0,4	0,0	0,1	0,0	0,3	0,0	-0,4	-0,4	0,3	-0,2	-0,3	0,4	-0,4	-0,4	-0,4	-0,2	0,5	0,5	-0,5	-0,1	-0,3	0,1	0,5	-0,3	0,2	0,0	-0,2	-0,2	0,0	0,1	-0,1	0,3	-0,7	0,0	-0,1	0,0	0,0	-0,2	0,0	-0,1	-0,2	-0,2	-0,1	-0,2	0,6
Paleogene. Upper Oligocene	-0,4	0,0	0,1	0,0	0,2	-0,1	-0,5	-0,5	0,3	-0,2	-0,3	0,2	-0,5	-0,3	-0,5	-0,2	0,4	0,5	-0,5	-0,1	-0,4	0,1	0,5	-0,2	0,2	-0,1	-0,3	-0,3	0,2	0,0	-0,2	0,3	-0,6	0,0	-0,1	0,0	-0,1	-0,2	0,0	-0,2	-0,2	-0,3	-0,3	-0,2	0,6
Cretaceous.Coniacian - Campanian	-0,3	0,0	0,0	-0,1	0,1	-0,1	-0,5	-0,2	0,2	-0,3	-0,2	0,3	-0,4	-0,3	-0,2	-0,3	0,3	0,3	-0,4	-0,1	-0,2	0,2	0,4	-0,3	0,0	0,0	-0,3	-0,1	0,0	0,1	-0,3	0,3	-0,6	-0,2	-0,1	-0,1	-0,1	-0,2	0,0	0,0	-0,2	-0,2	-0,1	0,0	0,4
Neogene. Lower -Middle Miocene	-0,2	0,1	-0,2	-0,3	-0,2	0,0	-0,1	-0,3	-0,1	0,0	0,0	0,3	-0,1	-0,7	0,1	-0,7	0,1	0,2	0,0	0,2	0,0	-0,3	0,1	0,0	-0,2	0,4	0,1	-0,1	-0,1	-0,4	-0,2	0,1	-0,4	-0,2	0,3	0,3	0,2	0,3	0,3	-0,3	0,1	0,0	-0,4	0,1	0,2
Upper Pliocene-Eopleistocene	-0,2	0,4	0,1	0,0	0,1	0,1	-0,3	-0,3	0,1	0,1	-0,1	0,4	-0,2	-0,5	-0,2	-0,3	0,4	0,3	-0,2	0,1	-0,1	0,1	0,4	-0,1	0,1	0,2	-0,1	-0,1	0,0	0,1	-0,1	0,2	-0,4	0,0	0,1	0,2	0,1	0,1	0,3	0,0	0,2	-0,2	0,2	0,1	0,3
Cretaceous.Cenomanian - Turonian	-0,3	0,0	0,0	-0,1	0,1	-0,1	-0,5	-0,2	0,2	-0,3	-0,2	0,3	-0,4	-0,3	-0,2	-0,3	0,3	0,3	-0,4	-0,1	-0,2	0,2	0,4	-0,3	0,0	0,0	-0,3	-0,2	0,0	0,1	-0,3	0,3	-0,6	-0,2	-0,1	-0,1	-0,1	-0,2	0,0	0,0	-0,2	-0,3	-0,1	0,0	0,4
Neogene. Lower Miocene	0,2	-0,2	-0,1	0,1	0,0	-0,5	0,1	-0,5	0,2	-0,2	-0,3	0,0	-0,5	-0,2	-0,2	-0,2	0,0	-0,1	-0,3	0,0	-0,2	-0,4	-0,2	0,4	0,0	0,1	-0,4	-0,3	0,1	-0,1	-0,6	-0,2	-0,2	0,0	0,1	0,0	0,0	0,1	-0,3	-0,4	0,2	-0,4	-0,8	-0,2	0,2

Table S3. Pairwise Pearson correlations of major and trace element concentrations in the Ket River (main stem and tributaries) during summer baseflow and main hydrochemical parameters of the water column and land cover. Significant ($p < 0.05$) correlations are given in red and most significant ($p < 0.01$) are highlighted in pink.

Table S4. Hydrochemical parameters of the Taz River basin (stem and tributaries), July 2019.

Parameter	main stem	tributaries	Element	main stem	tributaries
T_{water}, °C	18.8±0.65	18.7±1.71	Ge, µg L^{-1}	0.06±0.01	0.07±0.02
pH	6.87±0.33	6.76±0.37	As, µg L^{-1}	1.18±0.04	1.4±0.39
O_2, mg L^{-1}	8.4±0.89	7.11±2.37	Se, µg L^{-1}	0.04±0.003	0.04±0.01
SC, µS cm^{-1}	60.4±12.6	58.7±25.4	Rb, µg L^{-1}	0.67±0.16	0.56±0.19
TBC, *10^5 cells ml^{-1}	15.8±5.83	17.5±10.2	Sr, µg L^{-1}	24.7±4.93	22.4±5.7
Cl^-, mg L^{-1}	0.17±0.08	1.37±2.49	Y, µg L^{-1}	0.27±0.07	0.25±0.12
SO_4^{2-}, mg L^{-1}	0.69±0.16	0.68±0.52	Zr, µg L^{-1}	0.13±0.02	0.16±0.06
DIC, mg L^{-1}	6.16±1.67	5.73±2.83	Nb, µg L^{-1}	0.003±0.0005	0.003±0.001
DOC, mg L^{-1}	12.7±0.68	13.2±3.36	Mo, µg L^{-1}	0.12±0.05	0.19±0.35
PON, mg L^{-1}	0.36±0.07	0.44±0.31	Cd, µg L^{-1}	0.004±0.003	0.007±0.006
POC, mg L^{-1}	5.01±0.51	6.98±3.43	Sn, µg L^{-1}	0.005±0.001	0.005±0.002
$SUVA_{254}$, L mg C^{-1} m^{-1}	4.73±0.16	4.89±0.43	Sb, µg L^{-1}	0.02±0.003	0.03±0.01
P-PO_4, µg L^{-1}	41.5±8.53	42.2±25.9	Te, µg L^{-1}	0.004±0.003	0.004±0.002
N-NO_3, µg L^{-1}	2.56±0.27	3.66±2.05	Cs, µg L^{-1}	0.0007±0.0003	0.001±0.001
N-NO_2, µg L^{-1}	155±12.9	184±50	Ba, µg L^{-1}	4.16±0.54	4.25±1.26
N-NH_4, µg L^{-1}	17.2±2.25	35.5±21.3	La, µg L^{-1}	0.17±0.05	0.15±0.07
$N_{tot.}$, µg L^{-1}	337±43.2	357±68.3	Ce, µg L^{-1}	0.31±0.09	0.33±0.17
Li, µg L^{-1}	0.65±0.02	0.76±0.25	Pr, µg L^{-1}	0.05±0.01	0.04±0.02
Be, µg L^{-1}	0.014±0.002	0.02±0.007	Nd, µg L^{-1}	0.19±0.05	0.17±0.08
B, µg L^{-1}	5.91±0.39	7.65±3.66	Sm, µg L^{-1}	0.05±0.01	0.05±0.02
Na, mg L^{-1}	1.57±0.23	2.43±2.43	Eu, µg L^{-1}	0.01±0.003	0.01±0.004
Mg, mg L^{-1}	2.48±0.49	2.39±0.91	Gd, µg L^{-1}	0.05±0.01	0.05±0.02
Al, µg L^{-1}	44.6±45.2	41±18.4	Tb, µg L^{-1}	0.007±0.002	0.006±0.003
Si, mg L^{-1}	3.38±0.89	3.46±1.46	Dy, µg L^{-1}	0.04±0.01	0.04±0.02
P, µg L^{-1}	123±13.6	147±79.7	Ho, µg L^{-1}	0.01±0.002	0.008±0.003
K, µg L^{-1}	295±31.2	297±100	Er, µg L^{-1}	0.03±0.01	0.02±0.01
Ca, mg L^{-1}	5.91±1.32	5.18±1.96	Tm, µg L^{-1}	0.004±0.0008	0.003±0.001
Sc, µg L^{-1}	0.06±0.008	0.06±0.01	Yb, µg L^{-1}	0.02±0.005	0.02±0.009
Ti, µg L^{-1}	0.89±0.19	1.01±0.32	Lu, µg L^{-1}	0.003±0.001	0.003±0.001
V, µg L^{-1}	1.03±0.17	0.87±0.24	Hf, µg L^{-1}	0.004±0.001	0.005±0.002
Cr, µg L^{-1}	0.34±0.03	0.39±0.08	W, µg L^{-1}	0.002±0.0004	0.004±0.003
Mn, µg L^{-1}	24.5±16.7	107±90.8	Tl, µg L^{-1}	0.002±0.004	0.005±0.01
Fe, mg L^{-1}	0.75±0.12	0.96±0.5	Pb, µg L^{-1}	0.05±0.01	0.06±0.02
Co, µg L^{-1}	0.08±0.02	0.33±0.21	Bi, µg L^{-1}	0.005±0.005	0.008±0.01
Ni, µg L^{-1}	1.2±0.27	1.43±0.55	Th, µg L^{-1}	0.01±0.003	0.02±0.01
Cu, µg L^{-1}	0.85±0.18	0.86±0.49	U, µg L^{-1}	0.01±0.003	0.01±0.01
Zn, µg L^{-1}	2.62±0.97	3.96±2.55			
Ga, µg L^{-1}	0.03±0.009	0.03±0.01			

Preprints (www.preprints.org) | NOT PEER-REVIEWED | Posted: 30 June 2022 doi:10.20944/preprints202206.0422.v1

Table S5. Pearson pairwise correlations of major and trace elements of the river water (Taz and tributaries) with landscape parameters, vegetation coverage and climate.

Environmental parameter	pH	S.C.	Cl	SO_4	DIC	DOC	P_{tot}	NO_2	NO_3	NH_4	N_{tot}
$S_{watershed}$	0.18	-0.12	-0.17	-0.12	-0.05	-0.06	-0.14	-0.16	0.07	-0.29	-0.20
Dark Needleleaf	-0.34	-0.45	-0.40	-0.47	-0.33	0.29	0.40	0.07	0.30	0.08	**0.51**
Light coniferous and broadleaf mixed	-0.43	-0.36	-0.35	-0.48	-0.24	0.60	0.39	0.71	0.69	0.40	0.00
Decid Needleleaf	0.19	0.14	-0.49	-0.33	0.35	0.45	0.36	-0.15	0.15	0.07	0.03
Tundra	0.39	0.41	0.77	0.84	0.16	-0.72	-0.77	-0.44	-0.78	-0.39	-0.45
Riparian	-0.11	0.07	0.38	0.32	-0.11	-0.05	-0.54	-0.43	-0.58	-0.42	0.04
Bogs and Water	-0.26	-0.28	-0.23	-0.33	-0.26	-0.02	0.19	-0.02	0.09	0.03	0.61
Burns	-0.01	-0.15	-0.22	-0.17	-0.05	0.01	-0.17	-0.18	0.00	-0.41	-0.27
Phytomass	0.05	-0.01	-0.48	-0.38	0.19	0.40	0.13	-0.25	0.09	-0.24	-0.22
Org. C in soil, 0-30 cm	-0.17	-0.05	0.10	0.07	-0.09	-0.07	-0.22	-0.04	-0.08	-0.17	-0.09
Org. C in soil, 0-100 cm	-0.21	-0.08	0.08	0.01	-0.11	-0.06	-0.27	-0.05	-0.10	-0.22	-0.14
Permafrost	-0.17	-0.15	-0.21	-0.12	-0.08	-0.02	-0.06	-0.26	-0.13	-0.42	-0.13
	Si	Li	Be	B	Na	Mg	Al	Si	P	K	Ca
$S_{watershed}$	0.37	0.00	0.23	-0.10	-0.16	-0.08	-0.06	-0.17	-0.19	-0.15	-0.04
Dark Needleleaf	0.00	-0.09	0.11	-0.37	-0.41	-0.36	0.49	-0.44	-0.16	-0.14	-0.29
Light coniferous and broadleaf mixed	0.12	-0.41	0.43	-0.37	-0.40	-0.36	0.36	0.17	0.25	-0.59	-0.16
Decid Needleleaf	0.74	-0.55	-0.22	-0.22	-0.31	0.47	0.06	0.06	0.42	-0.56	0.60
Tundra	-0.33	0.69	-0.25	0.62	0.70	0.12	-0.36	0.37	-0.25	0.74	-0.06
Riparian	-0.75	0.45	0.12	0.05	0.13	-0.01	-0.05	-0.02	-0.27	0.33	-0.05
Bogs and Water	-0.64	-0.08	0.11	-0.23	-0.24	-0.19	0.02	-0.65	-0.24	0.06	-0.27
Burns	0.38	-0.01	0.20	-0.14	-0.20	-0.11	0.28	-0.17	-0.14	-0.08	-0.04
Phytomass	0.85	-0.41	0.01	-0.29	-0.36	0.27	0.27	-0.04	0.22	-0.51	0.41
Org. C in soil, 0-30 cm	-0.40	0.05	0.53	0.02	0.06	-0.20	-0.11	0.04	-0.11	0.19	-0.17
Org. C in soil, 0-100 cm	-0.39	0.05	0.58	0.00	0.05	-0.23	-0.07	0.03	-0.08	0.16	-0.19
Permafrost	0.26	-0.11	0.05	-0.21	-0.20	-0.10	0.27	-0.19	-0.16	-0.02	-0.03
	Sc	Ti	V	Cr	Mn	Fe	Co	Ni	Cu	Zn	Ga
$S_{watershed}$	0.15	-0.36	-0.26	-0.33	-0.26	-0.17	-0.32	-0.32	-0.24	-0.30	0.24
Dark Needleleaf	-0.17	0.00	-0.17	-0.08	-0.16	0.04	-0.06	-0.26	-0.30	-0.15	0.29
Light coniferous and broadleaf mixed	0.45	-0.22	-0.55	0.12	0.45	0.56	0.21	-0.67	-0.69	-0.17	-0.04
Decid Needleleaf	0.04	0.03	0.02	-0.05	-0.20	0.09	-0.15	-0.35	-0.36	-0.37	-0.37
Tundra	-0.14	-0.17	0.21	0.03	-0.14	-0.43	-0.30	0.58	0.61	0.32	0.20
Riparian	-0.08	-0.17	-0.21	-0.02	0.03	-0.10	0.09	0.55	0.43	0.09	0.29
Bogs and Water	-0.25	0.46	0.25	-0.07	0.00	-0.01	0.40	0.18	0.18	0.14	0.03
Burns	0.10	-0.20	-0.03	-0.31	-0.36	-0.12	-0.44	-0.27	-0.22	-0.34	0.34
Phytomass	0.15	-0.07	-0.07	-0.14	-0.32	0.06	-0.32	-0.39	-0.41	-0.41	-0.05
Org. C in soil, 0-30 cm	0.49	0.02	-0.05	0.01	0.49	0.18	0.49	0.03	0.04	0.37	0.02
Org. C in soil, 0-100 cm	0.52	0.01	-0.08	0.00	0.50	0.21	0.48	-0.01	-0.01	0.37	0.06

Table S5, continued.

Preprints (www.preprints.org) | NOT PEER-REVIEWED | Posted: 30 June 2022 doi:10.20944/preprints202206.0422.v1

	Ge	As	Se	Rb	Sr	Y	Zr	Nb	Mo	Cd	Sb
$S_{watershed}$	-0.33	-0.42	0.19	-0.13	0.00	-0.12	-0.29	-0.21	-0.15	0.17	0.06
Dark Needleleaf	-0.05	-0.33	-0.34	0.51	-0.27	-0.06	0.06	0.15	-0.25	-0.04	-0.35
Light coniferous and broadleaf mixed	0.18	0.15	-0.28	-0.37	-0.07	-0.39	-0.52	-0.21	0.49	0.74	0.16
Decid Needleleaf	-0.06	0.30	-0.25	-0.13	0.53	-0.25	0.06	0.22	-0.38	-0.29	-0.59
Tundra	0.07	-0.30	0.45	0.05	-0.12	0.47	0.13	-0.33	-0.08	-0.26	0.32
Riparian	0.21	-0.27	0.43	0.19	0.11	0.33	0.00	-0.12	0.08	0.03	0.40
Bogs and Water	-0.20	0.09	-0.10	0.31	-0.22	-0.07	0.27	0.46	0.05	-0.08	-0.02
Burns	-0.12	-0.42	0.04	0.16	0.03	-0.02	-0.22	-0.15	-0.17	0.09	-0.03
Phytomass	-0.03	0.01	-0.15	-0.01	0.40	-0.17	-0.04	0.11	-0.34	-0.11	-0.43
Org. C in soil, 0-30 cm	0.15	-0.15	0.21	0.14	-0.07	-0.04	-0.06	-0.09	0.84	0.59	0.54
Org. C in soil, 0-100 cm	0.16	-0.15	0.21	0.15	-0.09	-0.05	-0.09	-0.12	0.84	0.64	0.55
Permafrost	-0.05	-0.33	-0.08	0.34	-0.03	0.08	-0.12	-0.14	-0.16	-0.09	-0.14

	Cs	Ba	La	Ce	Hf	W	Pb	Bi	Th	U
$S_{watershed}$	0.09	0.06	0.31	0.50	-0.25	-0.35	0.05	0.28	-0.17	-0.15
Dark Needleleaf	-0.03	0.37	0.27	0.31	0.14	-0.47	0.17	-0.09	0.34	-0.27
Light coniferous and broadleaf mixed	-0.08	0.58	-0.18	-0.01	-0.38	0.02	0.14	0.75	-0.20	-0.68
Deciduos Needleleaf	0.63	0.18	-0.22	-0.30	0.20	0.03	-0.25	-0.24	-0.01	-0.27
Tundra	-0.16	-0.65	0.24	0.17	-0.09	0.24	-0.33	-0.27	-0.20	0.59
Riparian	-0.15	0.06	0.24	0.20	-0.03	-0.28	0.08	0.04	0.01	0.37
Bogs and Water	-0.27	0.12	-0.04	-0.03	0.29	-0.28	0.51	-0.12	0.44	0.10
Burns	-0.07	0.15	0.41	0.49	-0.18	-0.32	0.16	0.17	-0.07	-0.10
Phytomass	0.45	0.26	0.09	0.08	0.09	-0.20	-0.06	-0.04	0.01	-0.28
Org. C in soil, 0-30 cm	-0.16	0.05	-0.14	-0.10	-0.05	0.25	0.22	0.57	0.00	-0.02
Org. C in soil, 0-100 cm	-0.21	0.08	-0.11	-0.04	-0.08	0.22	0.25	0.62	0.00	-0.06
Permafrost	-0.04	0.07	0.33	0.28	-0.07	-0.33	0.06	-0.04	-0.03	-0.03

Preprints (www.preprints.org) | NOT PEER-REVIEWED | Posted: 30 June 2022 doi:10.20944/preprints202206.0422.v1

Table S6. Results of PCA of ~65 hydrochemical abd 16 land cover variables in ~ 60 sampling points of the main stem and tributaries of the Ket and Taz River basin, collected during summer baseflow.

	Factor 1	Factor 2	Factor 3
pH	-0.26	-0.26	-0.74
O_2	0.23	0.23	-0.31
Cond	-0.47	0.14	-0.81
Bact	-0.06	-0.63	0.05
Cl	0.00	-0.44	-0.14
SO_4	0.80	0.14	-0.32
DIC	-0.53	0.13	-0.76
DOC	0.49	0.52	0.29
PON	-0.42	-0.17	-0.51
POC	-0.43	-0.31	-0.38
SUVA	-0.27	-0.44	0.26
Li	-0.20	0.35	-0.54
Be	0.81	0.24	0.16
B	-0.21	0.09	-0.33
Na	-0.08	-0.72	-0.06
Mg	-0.13	-0.92	0.04
Al	0.76	0.44	0.24
Si	-0.14	-0.90	0.04
P	-0.32	-0.62	-0.01
Ca	-0.15	-0.90	0.05
Sc	-0.06	0.07	-0.58
Ti	0.84	0.13	-0.11
V	0.46	-0.66	-0.11
Cr	0.81	0.13	0.15
Mn	-0.39	-0.13	-0.17
Fe	-0.15	-0.82	0.13
Co	0.07	-0.22	0.07
Ni	0.22	0.18	0.05
Cu	0.76	-0.03	-0.07
Zn	0.09	0.43	0.28
Ga	0.91	0.16	0.15
Ge	0.55	-0.40	0.26
As	-0.37	-0.34	-0.09
Se	0.83	0.21	-0.37
Rb	0.03	0.49	0.15
Sr	-0.44	0.34	-0.73
Y	0.94	-0.15	0.07
Zr	0.90	0.09	-0.17

	Factor 1	Factor 2	Factor 3
Nb	0.81	0.31	-0.04
Mo	-0.32	-0.11	-0.29
Cd	0.39	0.35	0.34
Sb	0.76	0.35	0.11
Cs	0.22	0.17	-0.17
Ba	-0.02	0.78	-0.48
La	0.84	0.11	0.17
Ce	0.90	0.13	0.25
Pr	0.95	0.05	0.17
Nd	0.96	0.01	0.16
Sm	0.97	-0.01	0.13
Eu	0.94	0.05	0.12
Gd	0.97	-0.04	0.09
Dy	0.97	-0.06	0.08
Ho	0.98	-0.07	0.04
Er	0.97	-0.09	0.04
Yb	0.95	-0.09	0.05
Lu	0.96	-0.08	-0.04
Hf	0.91	0.20	-0.13
W	-0.09	-0.07	-0.17
Tl	0.22	0.01	-0.20
Pb	0.31	0.23	0.03
Bi	0.28	0.26	-0.23
Th	0.78	0.32	0.18
U	0.25	0.16	-0.72
$S_{watershed}$	0.07	-0.17	0.06
Dark Needleleaf	-0.12	0.55	0.04
Light Needleleaf	-0.28	0.74	0.34
Broadleaf	0.34	0.09	-0.39
Mixed	0.10	-0.20	-0.10
Riparian	-0.10	0.19	-0.14
Bogs	-0.08	-0.54	0.11
Water	-0.02	-0.49	0.09
Recent Burns	-0.14	0.30	0.29
Phytomass	0.06	0.88	-0.12
Rocks > 50 My	0.03	-0.21	0.06
Rocks 50-25 My	0.01	-0.18	0.10
Rocks < 25 My	0.12	0.78	0.13
Precipitation	-0.29	-0.20	0.51
MAAT	0.02	0.97	-0.10
Expl.Var	**26.28**	**13.67**	**6.56**
Prp.Totl	**0.31**	**0.16**	**0.08**

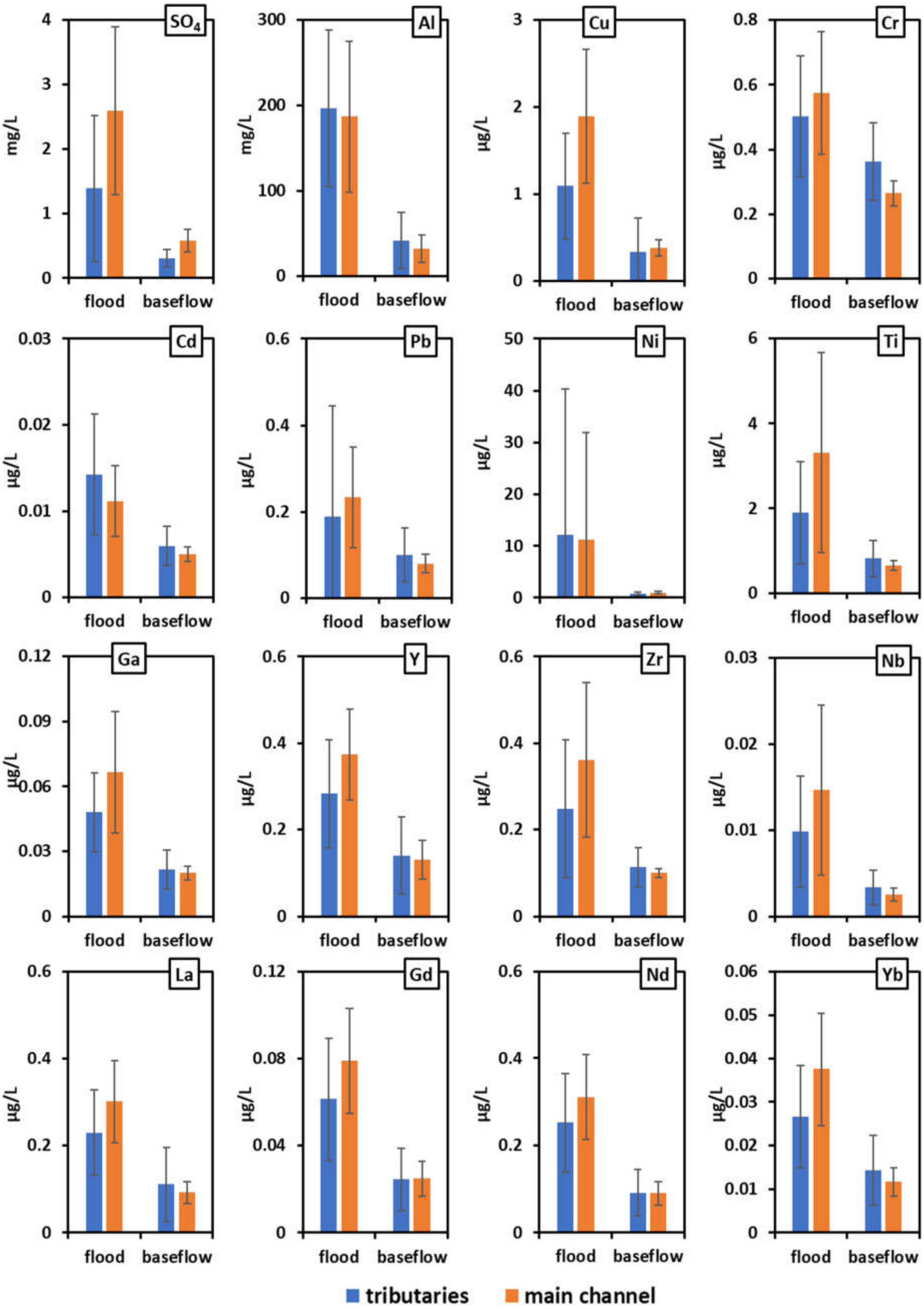

Fig. S1. Seasonal mean±SD concentration elements exhibiting higher concentrations during spring flood compared to summer baseflow in tributaries and main channel Ket′ in spring flood (blue) and summer (early fall) baseflow (orange).

doi:10.20944/preprints202206.0422.v1

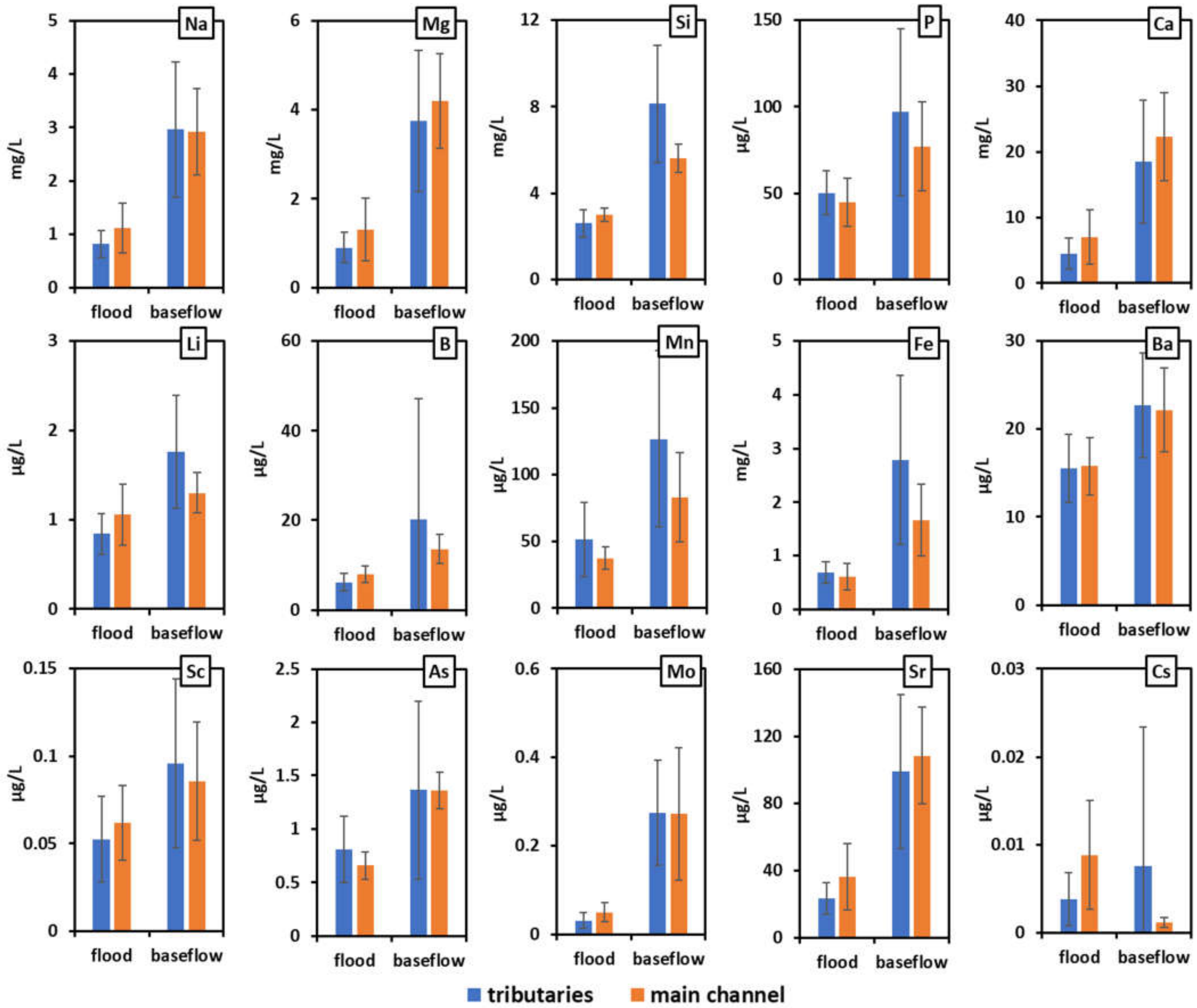

Fig. S1, continued. Seasonal mean±SD concentration elements exhibiting lower concentrations during spring flood compared to summer baseflow in tributaries and main channel Ket' in spring flood (blue) and summer (early fall) baseflow (orange).

 doi:10.20944/preprints202206.0422.v1

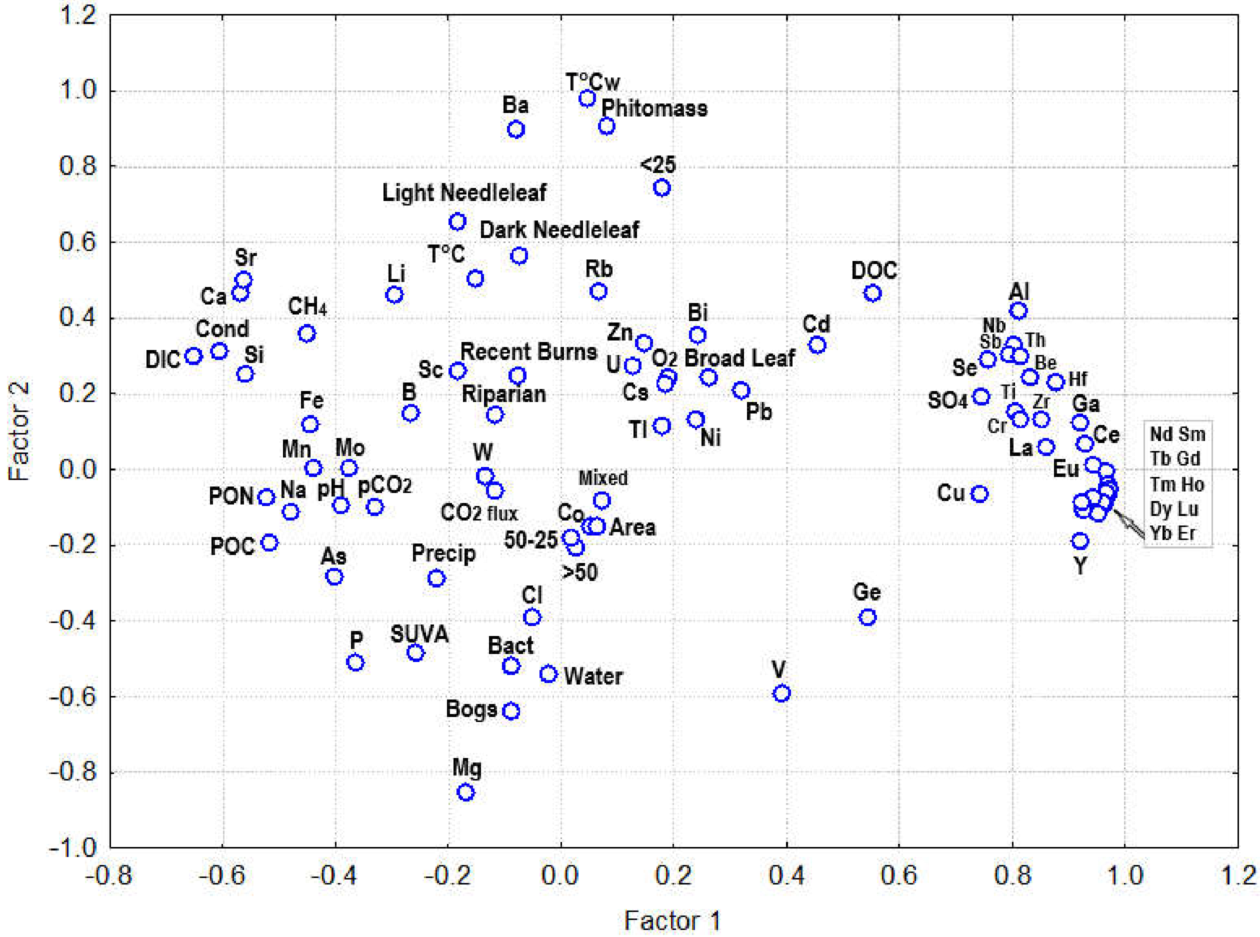

Fig S2. Results of PCA of ~65 hydrochemical abd 16 land cover variables in ~ 60 sampling points of the main stem and tributaries of the Ket and Taz River basin, collected during summer baseflow.